의학박사 학위논문

E prostanoid receptor 4 expressing macrophages mediate mucosal repair by production of Cxcl1 during colitis

E prostanoid receptor 4 를 발현하는 큰포식세포의 Cxcl1 생산을 통한 염증성 대장염의 점막회복 유도 기전 연구

2020 년 2 월

서울대학교 대학원
의학과 미생물학 전공
정 다 운

E prostanoid receptor 4 를 발현하는 큰포식세포의 Cxcl1 생산을 통한 염증성 대장염의 점막회복 유도 기전 연구

E prostanoid receptor 4 expressing macrophages mediate mucosal repair by production of Cxcl1 during colitis

February, 2020

The Department of Microbiology and Immunology in Seoul National University College of Medicine Graduate School

Daun Jung

ABSTRACT

E prostanoid receptor 4 expressing macrophages mediate mucosal repair by production of Cxcl1 during colitis

Daun Jung
The Department of Microbiology and Immunology
The Graduate School
Seoul National University

Restoration of epithelial barrier function prevents chronic inflammation upon facing intestinal microflora when tissue damages have occurred. Dysfunctional tissue regeneration is commonly considered to be a cause of inflammatory bowel diseases (IBDs). Macrophage is a fundamental component of wound healing, however, the key elements for generating a tissue regenerating phenotype of intestinal macrophage remain elusive. Here I found that E prostanoid receptor 4 (EP4) expression in macrophages is critically required for tissue regeneration in a damaged intestinal milieu. Csf1r-Cre/Esr1EP4$^{fl/fl}$ mice did not go through appropriate tissue regeneration with shortened colon length and prolonged disease activity index after recovery phase of dextran sodium sulfate induced colitis model. EP4^{+} macrophages are marked by high CD206 expression and high intracellular cAMP level at the resolution phase of colitis, implicating a functional significance

of EP4 in the formation of wound healing macrophages. RNA sequencing from sorted macrophages identified a Cxcl1 secreted from $EP4^+$ intestinal macrophages as a driving factor for the epithelial proliferation from regenerating crypts via the PGE_2/EP4/MAPK signaling axis. These studies thus define an important role of EP4 expression on intestinal macrophages to revive damaged epithelium.

Keywords: Inflammatory Bowel Diseases, E prostanoid receptor 4, macrophage, intestinal regeneration, C-X-C motif chemokine 1.

Student number: 2015-30542

CONTENTS

LIST OF TABLES AND FIGURES

LIST OF ABBREVIATIONS

Arg1: Arginase 1

BM: Bone-marrow

BMDC: Bone marrow-derived dendritic cell

BMDM: Bone marrow-derived macrophage

cAMP: Cyclic adenosine monophosphate

CD : Crohn's disease

CD-: Cluster of differentiation molecule

COX: Cyclooxygenase

CREB: cAMP response element-binding protein

C/EBPβ: CCAAT-enhancer-binding proteins beta

Cxcl1: C-X-C motif chemokine 1

DAI: Disease activity index

DC: Dendritic cell

Dpt: Days post DSS treatment

DSS: Dextran sodium sulfate

EC: Enterocyte

ELISA: Enzyme-linked immunosorbent assay

EP4: E prostanoid receptor 4

GM-CSF: Granulocyte macrophage colony stimulating factor

GOBP: Gene Ontology Biological Process.

HBSS: Hank's balanced salt solution

IBD: Inflammatory bowel diseases

IL-4: Interleukin-4

IL-10: Interleukin-10

KO: Knock out

M2: Alternatively activated macrophages

M-BMM: M-CSF grown bone marrow derived macrophage

M-CSF: Macrophage colony stimulating factor

MFI: Mean fluorescence intensity

MP: Macrophage

MPO: Myeloperoxidase

Mrc1: Macrophage mannose receptor 1

NSAID: Non-steroidal anti-inflammatory drug

PCR: Polymerase chain reaction

PGE_2: Prostaglandin E_2

PGs: Prostaglandins

PTGER4: Prostaglandin E2 receptor 4

Retnla: Resistin-like molecule alpha

RT: Room temperature

RT-PCR: Real time-polymerase chain reaction

TNF-α: Tumor necrosis factor-alph

INTRODUCTION

Intestinal mucosal healing is the final clinical criteria for the determination of complete remission in IBD patients (1, 2). Anatomical uniqueness of intestine renders mucosal healing as one of the most important requisites for the therapeutic effectiveness because of its role in preventing a direct contact between our body's immune system with the outside microbiota and food antigens (3, 4). During homeostasis, the epithelial barrier is maintained by highly active stem cells residing at the base of the crypts that provide continuous and perpetual cell renewal, with the majority of the differentiated cells being replaced every 3-5 days (5). However, in response to injury, additional mechanisms are rapidly implemented to restore the epithelial barrier. Delay or failure to do so can facilitate exposure to luminal antigens and potentially direct invasion of luminal microorganisms into the host, resulting in a heightened pro-inflammatory response, worsened tissue damage, and systemic infection. However, current standard therapies do not directly augment the mucosal healing, by contrast, they sometimes inhibit the natural process of mucosal healing by lowering several mediators inducing healing process at later sequences (2).

Among the many anti-inflammatory agents, non-steroidal anti-inflammatory drugs (NSAIDs) are contraindicated in gastrointestinal disorders (6). The first reason to be widely recognized why the NSAIDs aggravate intestinal lesion and abrogate wound healing is that NSAIDs have a mode of mechanism that block the action of cyclooxygenase-1 or –2 (COX-1/2) which produce prostaglandins (PGs) having many direct protective effects in maintaining enterocytes (ECs) homeostasis (7). Likewise, glucocorticoids, which reduce PGs synthesis by suppressing phopholipase A2, COX-2

and mPGES2 expression, adversely affect the wound healing of intestinal epithelium. Meanwhile, given that the mucosal healing process as a complex interaction between enterocytes and stromal cells, there are not sufficient works whether PGs augment the mucosal healing via the action on the stromal cells playing in the intestinal tissue repair other than enterocytes. Delineating the cellular and molecular mechanisms that modulate healing process via PGs provides an opportunity to identify detailed components that normally regulate the proliferative activities of epithelial progenitors. This hopefully will give a new approach to enhance therapeutic responses in IBD patients (Figure 1).

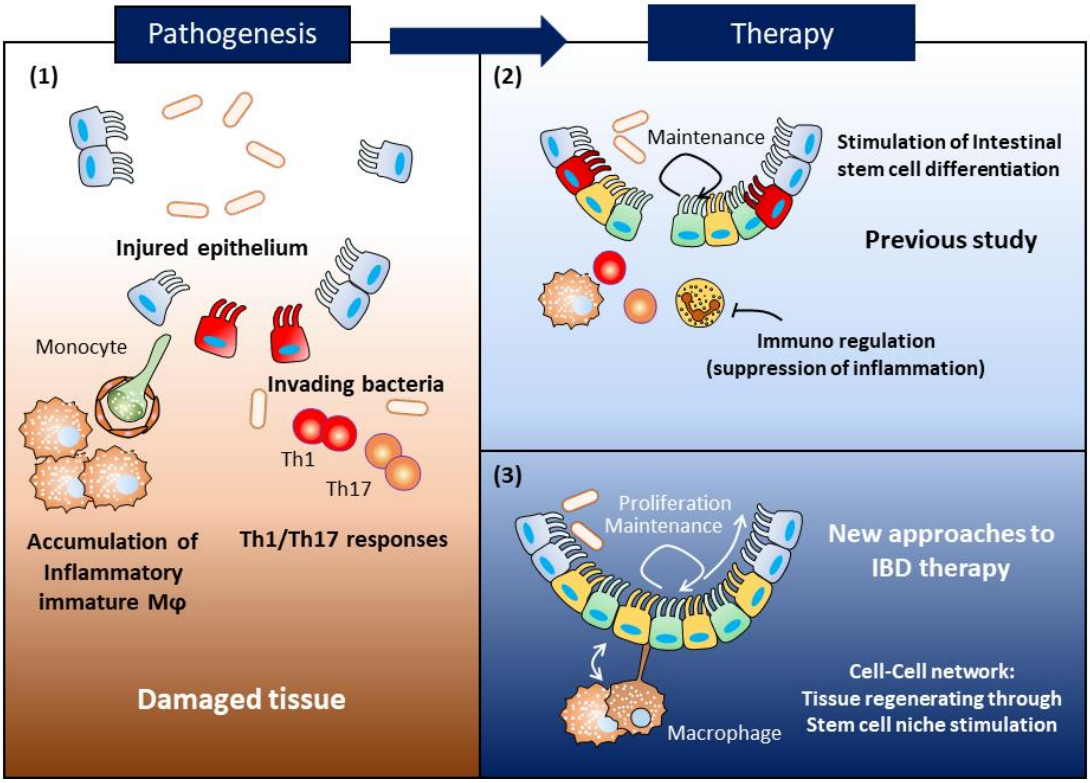

Figure 1. Inflammatory bowel disease pathogenesis and therapeutic approaches

Left panel: IBD pathogenesis (Injured epithelium, invading bacteria, Accumulation of immature macrophages, Increased Th1/Th7 responses) (1). Right panel: concepts of studies for IBD treatment. Previous studies focused on suppression of inflammation or stimulation of intestinal stem cell for IBD treatment (2). Advantages of new approaches (cell-cell network) have advantages that can regulate inflammation and at the same time stimulate epithelial proliferation (3). Cross-talk between macrophages and intestinal

stem cells in the intestine has implications for advances in regenerative medicine, and improved therapeutic strategies for inflammatory bowel disease.

Among the downstream lipid mediators of COXs, prostaglandin E_2 (PGE_2) has been known to have association with muscle and intestinal regeneration (8, 9). Majority of its effects were investigated on the parenchymal cells itself, in that PGE_2 expands skeletal muscle-specific stem cells via the E prostanoid receptor 4 (EP4) after injury by triggering a cyclic AMP (cAMP)/phopho CREB pathway that activates the proliferation inducing transcription factor, Nurr1(8). In intestine, PGE_2 induces differentiation of epithelial stem cells to wound-associated epithelial cells through EP4 (9). In case of skin, the effect of PGE_2 was recently reported in relation with M2 macrophage polarization and enhancing wound healing (10). However, its specific mode of action remains unclear and the exact actions of PGE_2 on the wound healing macrophages specifically in intestine still remain unresolved. In my previous study, endogenous PGE_2 contributed to the M2 characterization of resident macrophages, and promoted the pro-tumoral functions of tumor associated macrophages (TAMs) (11). Getting an idea from these and a study from Megan M *et al.* (12), showing the transcriptional similarities of wound healing macrophages with the TAMs, I hypothesized that PGE_2 is required for the wound healing function of intestinal macrophages. By using myeloid cell specific PGE_2 receptor knockout mice, I revealed in this study that E prostanoid receptor 4 (EP4) expressing macrophages was a critical component of colonic epithelial stem cell niche. They led the epithelial regeneration via production of Cxcl1 during colitis. EP4 was a potent, non-redundant receptor for the function of $CD206^+$ intestinal wound healing macrophages and was specifically required for the Cxcl1 synthesis during colitis, a previously unidentified molecule for a stem cell niche stimulation.

MATERIALS AND METHODS

Mice

Animal experiments were conducted in accordance to the Institute for Experimental Animals College of Medicine and cared for according to the Guide for the Care and Use of Laboratory Animals prepared by the Institutional Animal Care and Use Committee of Seoul National University (accession number SNU-171016-1-2). Male and female (10-12 weeks old) Csf1r-Cre (Tg(Csf1r-Mer-iCre-Mer)1Jwp strain) mice, Ai14 (Gt(ROSA)26Sor$^{tm14(CAG-tdTomato)Hze}$/J) mice, EP2 KO (Ptger2$^{tm1Brey/J}$) mice were purchased from Jackson Laboratory and Ptger4 floxed mice were kindly provided by Dr. Matthew Breyer (Eli Lilly and Company). *Csf1r-cre;Ptger4*$^{fl/fl}$ (Ptger4MϕKO) mice were generated by crossing Csf1r-Cre mice with Ptger4 floxed mice. Csf1r-Cre;Ai14 mice were generated by crossing Csf1r-Cre mice with Ai14 mice. For Csf1r specific EP4 ablation, tamoxifen (T5648; Sigma-Aldrich, St. Louis, MO, USA) is added to the diet as a tamoxifen-sucrose mixture. Csf1r specific EP4 knockout was achieved by feeding diet with 400 mg/kg tamoxifen with 5% sucrose to mice. Csf1r-Cre-Ai14 mice were injected with approximately 200 μl tamoxifen solution (200 mg/kg) once a day over 5 days. As control animals, co-housed and Cre-negative littermate mice were used in all experiments. All mice were housed in cages with a constant-flow air exchange supporting specific pathogen free condition. They were fed standard lab chow and they had access to water ad libitum.

Analysis of human microarray and RNA-seq data

All transcriptome data were retrieved from Gene Expression Omnibus (GEO) database (13). For microarray data, the series matrix files were downloaded and expression values were z-normalized for each sample. In the case of RNA-seq data, raw sequence read files

were downloaded and filtered by using fastp with default parameters (14). The remaining reads were then aligned to reference human transcriptome using kallisto to quantify expression levels (15).The reference human transcriptome annotation data (GRCh38.p13) were retrieved from GENCODE release 32 (16). Transcript-level expression values were merged into gene-level values by adding TPM values of all isoforms for each gene. Then, we used [Wilcoxon rank-sum test] to compare expression levels of PTGER4 between patients with ulcerative colitis and healthy controls.

DSS-induced colitis model

For induction of colitis, mice received one cycle (five days) of 2.5% DSS (MP Biomedicals, Santa Ana, CA, USA) in their drinking water. Animal weights were measured daily. Disease activity index (DAI) is the combined score of animal weight loss, stool consistency and bleeding present in the stool as described in Table 1. Mice were sacrificed at the indicated time points for futhur study.

Epithelial and lamina propria cell isolation

Colons were removed and washed in PBS. After removing all excess fat and faeces, the intestines were opened longitudinally, washed in Hank's balanced salt solution (Invitrogen, Carlsbad, CA, USA) containing 1% FBS, and cut into 0.5 cm sections. Tissue was incubated at 37°C shaking twice for 15min in HBSS (1mM EDTA,1% FBS) to remove the epithelial layer. Supernatant was collected and epithelial cells were obtained after centrifugation (5 min, 1,300 r.p.m.). Intestinal pieces were cut and incubated with pre-warmed 1.25 mg/ml collagenase D (Roche, IN 46256, USA), 0.85 mg/ml collagenase V (Sigma-Aldrich, St. Louis, MO, USA), 1 mg dispase (Invitrogen, Carlsbad, CA, USA), and 30 U/ml DNase (Roche, IN 46256, USA) in Minimum Essential Medium (MEM) α

Medium (Invitrogen, Carlsbad, CA, USA) containing 2 mM l-glutamine, 1% penicillin/streptomycin, 2-Mercaptoethanol, and 10% FBS for 30–45 min in a shaking incubator at 37 °C. The resulting cell suspension was passed through a 70 μm cell strainer (BD Falcon) and lamina propria cells were collected after centrifugation (10 min,1,500 r.p.m).

Generation of bone marrow derived macrophages

Bone marrow cells were obtained from Csf1r-Cre/Esr1 $EP4^{fl/fl}$ mice and differentiated into bone marrow derived macrophages (MPs) for 7 days in RPMI 1640 media containing 10% FBS, 1% penicillin/streptomycin, and 2 mM of L-glutamine (ThermoFisher Scientific, Waltham, MA 02451, USA), and supplemented with fresh recombinant murine M-CSF (50 ng/ml; Miltenyi Biotec, Bergisch Gladbach, Germany) and 4-Hydroxytamoxifen (6 μM; Sigma-Aldrich, St. Louis, MO, USA) every three days.

Adoptive transfer of bone marrow derived cells.

For adoptive transfer of dendritic cells (DCs), bone marrow cells were cultured in complete medium with recombinant GM-CSF (20 ng/ml; Miltenyi Biotec, Bergisch Gladbach, Germany) and IL-4 (5 ng/ml; Peprotech, Rocky Hill, NJ , USA). All cells were cultured at 37°C in a humidified incubator containing 5% CO_2. MPs were routinely > 95% F4/80+/CD11b+ cells and DCs were routinely > 40% $CD11c^{+}$ $CD11b^{int}$ MHC^{hi} cells. Cells were washed with PBS and transferred to *Csf1r-cre;Ptger4*$^{fl/fl}$ mice by intraperitoneal (IP) injection at 2×10^6 cells per mouse.

Quantitative Real-time PCR

For quantitative real-time PCR analysis, total RNA was solubilized in TRIzol reagent

(Invitrogen, Carlsbad, CA, USA) and extracted according to the manufacturer's instructions. cDNA was synthesized from 1 mg of total RNA using reverse transcription, and the amount of mRNA was determined using real-time PCR analysis with the SYBR Green qPCR Pre Mix (Enzynomics, Daejeon, Republic of Korea) on an ABI real-time PCR 7500 machine (Applied Biosystems, Foster City, CA, USA). Samples were normalized to TBP or 18S ribosomal RNA. The primer sequences are described in Table 2.

Western Blotting

Total cell lysates were prepared by harvesting cells in sample buffer (Biosesang, Seongnam, GG, Republic of Korea) with protease inhibitor and phosphatase inhibitor (GenDepot), sonicated for 40 s and heated to 99°C for 5 min. Proteins were resolved on 12% polyacrylamide gels and transferred to polyvinylidene difluoride membranes (Merck Millipore, burlington, MA, USA). The following Abs were used: anti–EP4 (101775; Cayman, Ann Arbor, MI, USA) and anti-β-actin (sc-47778; Santa Cruz Biotechnology, Dallas, TX, USA).

Flow cytometry

Following incubation with purified anti-CD16/CD32 for 10 mints at 4°C, $1x10^6$ cells were stained at 4°C in the dark using the antibodies listed in Table 3 and analyzed using an LSR II or FACS Aria I cytometer (BD Biosciences, San Jose, CA, USA) and FlowJo software (Treestar inc, Ashland, OG, USA). Intracellular staining was done after cell fixation and permeabilization (BD Biosciences, San Jose, CA, USA) followed by secondary Alexa Flour 488–conjugated goat anti-rabbit IgG (Invitrogen, Carlsbad, CA, USA) staining.

Histological Analysis

At autopsy, the length of the colon was measured and a section of colon was fixed with 4% paraformaldehyde and evaluated microscopically for inflammation indices by H&E staining. Histological scores of DSS-treated Csf1r-EP4$^{f-/-}$ mice were assessed by three indices: severity of inflammation (0 to 3), crypt damage (0 to 5), and ulceration (0 to 3).

Immunofluorescence staining

Frozen mouse colon tissues were sectioned to a thickness of 5 μm and fixed with ice-cold acetone for 10min. The tissue sections were incubated for 1h with blocking buffer (5% FBS, 0.3% Triton X-100 in PBS) at room temperature. The following primary antibodies were used: anti-F4/80 (MCA497GA; Bio-Rad, Hercules, CA, USA), anti-EP4 (101775; Cayman, Ann Arbor, MI, USA), anti-ki-67 (12202; Cell signaling, Danvers, MA, USA), anti-EpCAM (118207; Biolegend, Way San Diego, CA, USA), anti-Cxcl1 (MAB453; R&D systems, Minneapolis, MN, USA), anti-CD206. The tissue sections were incubated with primary antibodies overnight at 4°C in a humidified chamber. On the next day, appropriate secondary antibodies were applied, and nuclei were stained with 4,6-diamidino-2-phenylindole (DAPI, D8417; Invitrogen, Carlsbad, CA, USA) before mounting. Fluorescence signal was detected using a Leica TCS SP8 confocal microscope.

Immunohistochemistry

Tissues were fixed in 4% paraformaldehyde (Merck Millipore, burlington, MA, USA) in PBS for 1 day and sectioned at a thickness of 4.0 μm. Slides were deparaffinized, rehydrated, and antigen-retrieved in a citrate buffer (10 mM sodium citrate, 0.05% Tween 20, pH 6.0) for further analysis. Primary antibodies were pre-diluted in blocking buffer

to 1:200 for ki-67 (12202; cell signaling) and were applied to tissue sections overnight at 4°C in a humidified chamber. Biotinylated secondary antibodies were applied, followed by signal development with liquid DAB substrate (K3467; Dako). Sections were counterstained with hematoxylin (Merck Millipore, burlington, MA, USA). Imaging was performed using microscope (Eclipse Ci-L; NIKON)

ELISA

Colons were homogenized in Homogenization buffer (0.1M phosphate, pH 7.4, containing 1mM EDTA and 10 μM indomethacin) using TissueLyser (Qiagen, Valencia, CA, USA). IL-10, TNF-α, CXCL-1 in cell culture supernatants or colon lysate were measured using mouse Duoset ELISA kit (BD Biosciences, San Jose, CA, USA) according to the manufacturer's protocol. PGE_2 levels were measured using a PGE_2 ELISA Kit (Cayman, Ann Arbor, MI, USA)

Intestinal macrophage isolation and RNA Sequencing

To isolate intestinal macrophages from lamina propria cells, $CD45^+CD11b^+Ly6G^-Ly6C^-MHCII^+CD64^+$ intestinal macrophages were sorted using FACS AriaIII (BD Biosciences, San Jose, CA, USA) and prepared for further analysis. Sorting purity was assessed and confirmed to be up to 95-98%. Total RNA was extracted using TRIzol reagent (Invitrogen, Carlsbad, CA, USA) according to the manufacturer's instructions. For control and test RNAs, the construction of the library was performed using the QuantSeq 3' mRNA-Seq Library Prep Kit (Lexogen, Vienna, Austria) according to the manufacturer's instructions. High-throughput sequencing was performed using single-end 75 sequencing on a NextSeq 500 (Illumina, San Diego, CA, USA). QuantSeq 3' mRNA-Seq reads were aligned using Bowtie2 (Langmead and Salzberg, 2012). Bowtie2 indices were either

generated from genome assembly sequence or representative transcript sequences for aligning to the genome and transcriptome. The alignment file was used for assembling transcripts, estimating their abundances, and detecting differential expression of genes. Differentially expressed genes were determined based on counts from unique and multiple alignments using coverage in Bedtools (Quinlan AR, 2010). The RT (Read Count) data were processed based on the global normalization method using the Genowiz™ version 4.0.5.6 (Ocimum Biosolutions, Hyderabad, India). Gene classification was based on searches done by DAVID (http://david.abcc.ncifcrf.gov/) and Medline databases (http://www.ncbi.nlm.nih.gov/). Enriched terms that passed $P\text{-}value < 0.05$ were reported. All sequencing data can be found at the Gene Expression Omnibus (GEO) database (GSE141093).

Crypt isolation and in vitro organoids cultivation

Intestinal crypts were dissociated from mouse small intestine using Cell Dissociation buffer (0.5mM EDTA in PBS). Crypts were subsequently used for establishing organoids by cultivation in Matrigel (BD Biosciences, San Jose, CA, USA) and Intesticult medium (Stemcell Technologies). Briefly, crypts were re-suspended in Intesticult medium at 10^4 crypts/ml and mixed 1:1 with Matrigel. Next, 50 µl Matrigel plugs were plated in pre-warmed 24-well plates and allowed to settle, before addition of 750 µl of prewarmed Intesticult medium and subsequently cultured at 37 °C in a 5% CO_2 atmosphere. Next day, some wells were treated with either 5% culture supernatant of lamina propria cells isolated from WT and Csf1r-EP4$^{-/-}$mouse or 10 ng/ml recombinant Cxcl1 (Peprotech, Rocky Hill, NJ, USA). Fresh medium was replaced 4d of cultivation. After 7 days, intestinal organoids were analyzed for the efficiency of budding crypts and were used for Immunofluorescence staining. For Immunofluorescence staining of crypt organoids, ice

cold cell dissociation buffer was added to the wells and the organoids gently pipetted to disrupt the Matrigel plug. The organoids were then allowed to settle by gravity, the supernatant discarded and then washed 3 more times in ice cold PBS. The dissociated crypts were then allowed to settle by gravity, re-suspended in PBS and fixed with 4% paraformaldehyde.

Statistical analysis

Mann–Whitney U-test was used to determine statistical significance between groups using the GraphPad Prism Software v.6 (GraphPad, La Jolla, CA, USA). P-value of less than 0.05 was considered statistically significant, represented by $*P<0.05$, $**P<0.01$, $***P<0.001$ and $****P < 0.0001$.

RESULTS

Expression of E prostanoid receptor 4 is related with resolution of colitis

Although the genome-wide association studies have reported that the *PTGER4* gene, which encodes the PGE_2 receptor EP4, has a strong genetic association with both forms of IBD, the exact expression patterns of the *PTGER4* in the colitis have not been clarified. To further investigate the expression of EP4 in human patients, I first analyzed transcriptome data of human IBD samples and found significant downregulation of mRNA expression levels of the *PTGER4* in samples from both Crohn's disease (CD) and ulcerative colitis (UC) patients relative to those in healthy controls (Figure 2A-E). Furthermore, expression levels of the *PTGER4* in samples of UC patients under remission state were increased (Figure 2F-G). These results indicate that expression of the *PTGER4* is largely related with remission of IBD patients. These findings raise the question concerning which cell types highly express EP4 in colon tissues. In fact, EP4 is required for epithelial cell survival and is one of the most abundant and potent EP receptors expressed in Th17 cells, I found that macrophages are the cells that highly expressed EP4 in the colon. The expression of the EP4 was observed throughout the colon with enrichment on stromal cells in lamina propria (Figure 3A). Especially, EP4 was predominantly co-localized in the $F4/80^+$ macrophages in the colonic lamina propria (Figure 3B). To further investigate the expression of EP4, EP4 levels were analyzed using fluorescence-activated cell sorting (FACS) in lamina propria of mouse normal colon tissue. I found that the expression of EP4 was increased during differentiation from monocytes to mature macrophages (Figure 3D). Also, macrophages were highly expressing EP4 in immune cells in lamina propria (Figure 3C-D). Taken together, the

above results indicate that macrophages which are highly expressing EP4 in lamina propria of colon tissue may contribute to the resolution of intestinal inflammation.

Endogenous prostaglandin E_2 potentiates anti-inflammatory phenotype of macrophage through CREB-C/EBP-β cascade

Before I examine the role of PGE_2-EP4 signaling of macrophage in the resolution of colitis, I tested the initial hypothesis that PGE_2 is required for the wound healing function of macrophages. Through my previous study, I found that differentiating bone marrow derived macrophages (BMDMs) under the effect of M-CSF produce PGE_2 endogenously, resulting in anti-inflammatory gene expression upon differentiation induced by macrophage colony stimulating factor (11). COX inhibition by indomethacin reduced endogenous PGE_2 production of macrophages and subsequently reduced interleukin-10 (*Il10*), arginase (*Arg1*) and macrophage mannose receptor 1 (*Mrc1*) gene expressions (11). Consistent with my previous study, PGE_2 increased *Il10*, *Arg1*, and *Mrc1* gene expressions in macrophages (Figure 4A-C). Furthermore, my study identified that signaling by EP2 and EP4 is triggered by PGE_2 binding, and then adenylate cyclase is activated, leading to an increase in intracellular cAMP levels, which in turn activates Protein Kinase A (PKA). Activated PKA then causes phosphorylation of cAMP response element-binding protein (CREB). This leads to the transcription of CCAAT-enhancer-binding proteins beta (C/EBP-β) which promotes *Il10*, *Arg1*, and *Mrc1* gene expression (Figure 4D) (11). Collectively, endogenous PGE_2 promotes anti-inflammatory phenotype macrophage differentiation through the CREB/CEBP-β cascade.

Generation and characterization of Csf1r-cre;Ptger4$^{fl/fl}$ mice

To elucidate the role of EP4 of macrophages in resolution of colitis, I made myeloid cell

specific EP4 knockout mice. Mice carrying a floxed allele of *Ptger4* were crossed to *Csf1r-cre* mice to generate *Csf1r-cre;Ptger4*$^{fl/fl}$ mice that will have a deletion of *Ptger4* restricted to myeloid cells (Figure 5A). Analysis of BMDMs-derived DNA from the Ptger4$^{fl/fl}$ mice with or without cre showed efficient ablation of the 340 bp floxed allele in the presence of Csf1r-cre with 4-hydroxytamoxifen (4-oht) treatment (Figure 5B). Feeding tamoxifen (Tm) diet (250mg/kg) to these mice induced Csf1r specific *Ptger4* ablation as shown by genotyping on the *Ptger4* floxed allele from sorted CD115^{+} myeloid cells, CD45^{-}CD31^{+} endothelial cells and CD45^{-}EpCAM^{+} epithelial cells in colon. The presence of *Ptger4* floxed allele was detected in all the tissue samples except in the targeted myeloid cell (Figure 5C). In addition, RNA of exon2 of *Ptger4* was almost deleted and EP4 protein level was significantly decreased in sorted CD45^{+}CD11b^{+}Ly6G^{-} Ly6C^{-}MHCII^{+} macrophages from colon of *Csf1r-cre;Ptger4*$^{fl/fl}$ mice. (Figure 6A-B). But RNA of exon2 of *Ptger4* in epithelial cells from *Csf1r-cre;Ptger4*$^{fl/fl}$ mice was not different with WT (Figure 6C). Both RNA and protein of the WT versus *Csf1r-cre;Ptger4*$^{fl/fl}$ BMDMs indicated EP4 deletion (Figure 6D-E). The cAMP level was measured to EP4 signaling activity and this result showed that cAMP level of colonic macrophages from *Csf1r-cre;Ptger4*$^{fl/fl}$ mice was decreased than that of *Ptger4*$^{fl/fl}$ mice (Figure 6F). My previous study identified that mouse BMDMs express 4 types of PGE_2 receptors, EP1 to EP4 with similar expression levels (11). In accordance with this, I detected all types of EPs on the macrophages isolated from the lamina propria of mouse colon with no big difference of expression levels detected by flow cytometry (Figure 7A). Because both EP2 and EP4 induce intracellular cAMP accumulation which has relation with M2 genes induction including *Arg1*, *Mrc1* and resistin-like molecule alpha (*Retnla*) (11), I examined which EP receptor is a potent receptor for cAMP signaling. The cAMP levels of WT and EP2 KO BMDMs was significantly increased by PGE_2, however *Csf1r-*

cre;Ptger4$^{fl/fl}$ BMDMs did not respond to PGE_2 stimulation. From this result, EP4 was identified as the strongest receptor for PGE_2 that induced downstream cAMP signaling in macrophages (Figure 7B). In addition, analysis of endogenous Csf1r expression by crossing *Csf1r-cre* and Ai14 mice confirmed that Csf1r was specifically expressed in the monocytes, macrophages and dendritic cells as previously reported (Figure 8). About 45% of neutrophils and 43% of dendritic cells had tdTomato signal. In contrast, about 93% macrophages had that signal. This result indicated that cre-recombination event could mainly occur in macrophages in our mice.

Monocyte derived EP4$^+$ macrophages are essential for the mucosal repair during intestinal inflammation

Before exploring the role of macrophage EP4 signaling in mucosal immune responses, I first characterization dextran sodium sulfate (DSS) induced colitis model in normal B6 mice (Figure 9A). The body weight was decreased gradually until 7-8 days (inflammatory phase) and increased again until 20-25 days (resolution phase) (Figure 9B). Additionally, mice exhibited a significant increase in disease activity index (DAI) (Figure 9C), shortened colon length (Figure 9D) and increased histology score (Figure 9E) in the inflammatory phase. IBD is characterized by the infiltration and activation of various immune cells, leading to prolonged inflammation in the intestine. In order to identify the colonic cellular populations involved in acute and chronic DSS-induced colitis, Lamina propria (LP) leukocyte cells isolated from DSS-treated mice were examined. Similar to the body weight result (Figure 9B), I observed a significant increase in the number of $CD45^+$ leukocytes in lamina propria until day 8 (Figure 10A). The number of Neutrophils peaked at day5 and was gradually decreased until day 28 (Figure 10B). An identical "waterfall" of $Ly6C^{hi}$ monocytes developing progressively into $CD64^+Ly6C^-MHCII^+$

mature macrophages in resting mouse intestine has also been proposed in a recent study (17). In that study, inflammation alters monocyte-macrophage differentiation, causes selective accumulation of both Ly6C^{hi} monocytes and intermediates and decreased mature macrophage. In accordance with these reports, the number of monocytes (Figure 10C) and intermediates (Figure 10D) was increased in the inflammatory phase. In contrast, the number of mature macrophages was decreased during the inflammatory phase and gradually increased until day 28 (Figure 10E). Collectively, these results show that my DSS colitis model is well characterized with previously reported features.

To compare any gross difference of inflammatory phenotype between *Ptger4*$^{fl/fl}$ and *Csf1r-cre;Ptger4*$^{fl/fl}$ mice, I induced colitis by providing 2.5% DSS containing water for 5 days. The recovery phase was followed for 12~33 days until *Ptger4*$^{fl/fl}$ mice re-gained original weights. Interesting result was found in the body weight curve, in that *Ptger4*$^{fl/fl}$ mice started to increase their weights from 7 days post DSS treatment (dpt) and almost recovered by 19 dpt, in contrast, *Csf1r-cre;Ptger4*$^{fl/fl}$ mice did not gain weight and stayed around 85% of starting point by 19 dpt (Figure 11A-B). This data directly connected to the DAI which scores the extent of bloody stool, consistency of stool in addition to the weight loss (Figure 11C). *Ptger4*$^{fl/fl}$ mice showed the highest DAI score by 5~7 dpt and revered to near homeostatic level, however, *Csf1r-cre;Ptger4*$^{fl/fl}$ mice showed delayed recovery of symptoms and stayed to the score of 4 by 19 dpt. Next, I sacrificed mice at each time point and observed colon length (Figure 11D). The length of the colon went similar with the weight curve in that *Ptger4*$^{fl/fl}$ mice had the most shortened colon by day 5 and consistently lengthen colon till the day 28. Notably, *Csf1r-cre;Ptger4*$^{fl/fl}$ mice were evident to have uniformly short colons during the whole recovery phase.

Next, I determined whether the defect of normal recovery was come out from more severe extent of early inflammation in *Csf1r-cre;Ptger4*$^{fl/fl}$ mice. Distinct from whole cell EP4$^{-/-}$ mice which showed a significantly severe form of colitis from the initiation phase (), myeloid cell specific EP4 knockout induced a similar extent of inflammation as analyzed by myeloperoxidase (MPO) assay using the whole colon lysate (Figure 12A). Infiltrations of total leukocytes, neutrophils and monocytes were not significantly different, except the neutrophil counts by 5 dpt which were even lower in *Csf1r-cre;Ptger4*$^{fl/fl}$ compared to *Ptger4*$^{fl/fl}$ mice (Figure 12B-D). In accordance with this, histological scores were not different during the early inflammatory phase, whereas *Csf1r-cre;Ptger4*$^{fl/fl}$ mice showed significantly higher scores at later recovery phase due to the remnant of crypt loss and erosion, supporting the defect of the repair process in these mice (Figure 13).

To examine the contribution of Csf1r positive macrophages to the regenerating intestine, I adoptively transferred *Ptger4*$^{fl/fl}$ bone marrow derived macrophages (MPs) or dendritic cells (DCs), which were the major two populations expressing Csf1r in the mouse intestine, to the *Csf1r-cre;Ptger4*$^{fl/fl}$ recipient mice in total three rounds during recovery phase (Figure 14A-B). As expected, *Ptger4*$^{fl/fl}$ MPs, not DCs injection, led to lengthen colons of recipient mice, which predicts that EP4 expressing macrophages are important in regeneration (Figure 14C). Collectively, these findings demonstrate that monocyte derived EP4 expressing macrophages are required for the proper mucosal repair during an ECs damage induced intestinal inflammation.

EP4 expressing macrophages induce regenerative responses of the damaged intestinal epithelium

To examine more closely on the defect of repair in *Csf1r-cre;Ptger4*$^{fl/fl}$ mice, I quantified crypt numbers per unit length in colons from *Ptger4*$^{fl/fl}$ and *Csf1r-cre;Ptger4*$^{fl/fl}$ mice by 7 and 21 dpt. As a result, the number of crypts per 500 ㎛ was decreased by 7 dpt because of DSS mediated toxicity both in *Ptger4*$^{fl/fl}$ and *Csf1r-cre;Ptger4*$^{fl/fl}$ mice (Figure 15A). At 21 dpt however, *Ptger4*$^{fl/fl}$ mice showed a marked increase in the number of crypts, whereas *Csf1r-cre;Ptger4*$^{fl/fl}$ mice had significantly lower crypts compared to *Ptger4*$^{fl/fl}$, implicating the defect of the repair was relevant in a crypt regeneration. I next confirmed the Ki67^{+} epithelial cells which faithfully represent proliferating cells outward from crypt niche. Analysis by flow cytometry using isolated colonic epithelial cells (Figure 15B) and immunohistochemistry on fixed whole colons (Figure 15C) showed that proliferating epithelial cells in *Csf1r-cre;Ptger4*$^{fl/fl}$ mice was significantly lower compared to *Ptger4*$^{fl/fl}$ mice by 21 dpt in a resolution phase.

To explore a sequential crypt response during colitis, I identified the transcripts of each cellular components in the whole epithelium (Figure 16A). Following damage by 7 dpt, I found that all transcript markers for the crypt including Lgr5 (crypt-base columnar cells, CBCs), Bmi1 (reserve stem cells, RSCs), Muc2 (goblet cells) and Reg4/Lyz1/Lyz2 (deep crypt epithelial cells), were steeply decreased, representing the crypt loss as previously reported. From 14 dpt during regeneration, these genes were transcriptionally increased in *Ptger4*$^{fl/fl}$ mice, whereas remained low in *Csf1r-cre;Ptger4*$^{fl/fl}$ mice at 21 dpt or 35 dpt (Figure 16B-C). Because the CBCs and RSCs are known to drive the turnover of the intestinal epithelium, these results demonstrate that EP4 expressing macrophages are required for the repair of the damaged intestine by probably supporting the regenerating function of intestinal stem cells and promoting epithelial proliferation.

Macrophage EP4 signaling promotes the wound healing function of colonic macrophages

Previously concept on tissue repair poised macrophages as a critical arm of tissue regenerating machinery. In the intestine, $CD206^+$ wound healing macrophages are known to participate in rebuilding damaged area (18, 19). Although IL-4 is the most powerful cytokine for inducing $CD206^+$ alternatively activated macrophages (20), it is still not certain whether this scenario also fit in the intestine. Before exploring the involvement of EP4 expression with the function of wound healing macrophages, I first confirmed the involvement of IL-4 in the formation of $CD206^+$ wound healing macrophages. I induced colitis in normal B6 mice by DSS treatment and followed the change in body weight with injection of IL-4 neutralizing antibody (nIL-4 Ab.) or corresponding isotype antibody three times a week throughout the whole recovery period (Figure 17A). Phosphorylation of Stat6 was decreased by nIL-4 (Figure 17B). Intriguingly, depletion of IL-4 did not affect the weight change during colitis, colon length by 25 dpt (Figure 17C), nor the development of $CD206^+$ macrophages (Figure 17D). Another marker expression for wound healing macrophages including Arg1, Retnlα and IL-10 were not all different between isotype and nIL-4 Ab. received mice (Figure 17E), demonstrating that IL-4 was not an important factor for inducing intestinal repair.

I next examined whether the EP4 expression contributed to the development of wound healing macrophages. As expected, by 39 dpt when the shortened colons were obviously observed in *Csf1r-cre;Ptger4*$^{fl/fl}$ mice (Figure 18A), decrease of $CD206^+$ (Figure 18B) as well as $Arg1^+$ and $Retnlα^+$ macrophages (Figure 18C) were shown in *Csf1r-cre;Ptger4*$^{fl/fl}$ mice whereas the mature macrophage population itself was not different (Figure 18D). Notably, I detected a strong positive correlation of EP4 expression with the CD206

expression in intestinal macrophages by flow cytometry (Figure 18E), all supporting the notion that the EP4 expression of macrophages is required for the intestinal regeneration via the formation of wound healing macrophages.

To define the mechanisms that underlie regeneration driven by $EP4^+$ macrophages, I transcriptionally compared the *Ptger4*$^{fl/fl}$ and *Csf1r-cre;Ptger4*$^{fl/fl}$ mature macrophages isolated from colon by 39 dpt. Total 252 genes were differentially identified in RNA sequencing data and further analyzed for the enriched gene ontology biological processes (GOBPs) using the upregulated gene set (Category 1) in *Ptger4*$^{fl/fl}$ compared to *Csf1r-cre;Ptger4*$^{fl/fl}$ macrophages (Figure 19A). As a result, wound healing signature including *Mrc1*, *Retnlα*, *Igf1r*, *Anxa5*, *Cxcr4*, *Csrp1*, *Prkc*a and *Arg1* was predominantly decreased in *Csf1r-cre;Ptger4*$^{fl/fl}$ macrophages (Figure 19B). Concomitantly, the regulation of multi-organ process, endothelial cell proliferation and tissue development were enriched in *Ptger4*$^{fl/fl}$ mice implicating the involvement of $EP4^+$ macrophages in maintaining tissue homeostasis (Figure 19C-E). Several genes involved in immune response were also identified as decreased in *Csf1r-cre;Ptger4*$^{fl/fl}$ macrophages, including *Cebpα*, *Cxcl1* and *Prkca* (Figure 19F). Collectively, these results demonstrated that EP4 expression governs the general feature of wound healing macrophages. Among the top significant transcripts, I next seek which molecule was directly involved in epithelial regeneration.

Cxcl1 production from EP4$^+$ macrophages is necessary for the intestinal epithelial regeneration

To investigate whether soluble factors derived from $EP4^+$ macrophages are relevant for the epithelial repair or not, I isolated lamina propria mononuclear cells (LPMC) of colon from WT mice and cultured overnight before collecting supernatants. Then the *Csf1r-*

cre;Ptger4$^{fl/fl}$ mice were received 300 μl of LPMC sup intraperitoneally total six times from 20 to 30 dpt (Figure 20A). Treatment with LPMC sup from *Ptger4*$^{fl/fl}$ colon significantly lengthen colons of *Csf1r-cre;Ptger4*$^{fl/fl}$ mice, revealing the soluble factors were involved in epithelial regeneration (Figure 20B). For the possible candidates, I chose Cxcl1, one of the most significantly different genes between *Ptger4*$^{fl/fl}$ and *Csf1r-cre;Ptger4*$^{fl/fl}$ macrophages and as a secretary molecule, for the major factor inducing epithelial regeneration given that its known function for stimulating cancer stem cell survival. As a result, Cxcl1 was exclusively detected in *Ptger4*$^{fl/fl}$ compared to *Csf1r-cre;Ptger4*$^{fl/fl}$ LPMC sup (Figure 20C). Cxcl1 was predominantly co-localized in the F4/80^{+} macrophages in the colonic lamina propria of *Ptger4*$^{fl/fl}$ mice (Figure 21A-B) as determined by immunofluorescence staining, whereas *Csf1r-cre;Ptger4*$^{fl/fl}$ mice barely showed Cxcl1 expression in colon. These data indicate that macrophages are the major producers of Cxcl1 in the resolution phase of colitis and the majority of Cxcl1 is derived from EP4 signaling.

To explore the direct effect of Cxcl1 in crypt regeneration, I isolated intestinal crypts from *Ptger4*$^{fl/fl}$ mice and cultured them in the matrigel with or without treatment of recombinant Cxc1. Surprisingly, 10 ng/ml of Cxcl1 obviously promoted epithelial regeneration as determined by crypt budding efficiency (Figure 22A-B) as well as the ratio of Ki67^{+} proliferating cells in the crypt (Figure 22C-E). Next, I treated LPMC culture medium (CM) to the regenerating crypts and confirmed higher budding efficiency in crypts cultured with CM from *Ptger4*$^{fl/fl}$ LPMC compared to *Csf1r-cre;Ptger4*$^{fl/fl}$ LPMC. Adding neutralizing antibodies for the Cxcl1(nCxcl1) in the CM of WT LPMC reverted the budding efficiency to the level of CM of *Csf1r-cre;Ptger4*$^{fl/fl}$ LPMC (Figure 23A-B). Similar with LPMC results, CM from *Csf1r-cre;Ptger4*$^{fl/fl}$ BMDMs decreased budding

efficiency in Crypts and nCxcl1 reverted effect of CM of WT BMDMs (Figure 23C-D). Collectively, these findings demonstrate that $EP4^{+}$ macrophages induce intestinal regeneration via stimulation of epithelial proliferation from crypt in a Cxcl1-dependent manner.

Cxcl1 is produced under the PGE_2/EP4/MAPKs signaling pathway in the wound healing macrophages

To define the exact molecular mechanisms of Cxcl1 production from macrophages, I first determined Cxcl1 gene transcripts in *Ptger4*$^{fl/fl}$ BMDMs with stimulation of 10 μM of PGE_2. At 48 hours post PGE_2 treatment, Cxcl1 mRNA was increased 30-fold (Figure 24A). Notably, this was primarily mediated by EP4, because only *Csf1r-cre;Ptger4*$^{fl/fl}$ BMDMs did not increase Cxcl1 production upon PGE_2 treatment whereas $EP2^{-/-}$ and WT BMDMs significantly increased Cxcl1 (Figure 24B). I next analyzed PGE_2 levels during colitis to examine a correlation between PGE_2 and Cxcl1 levels. PGE_2 itself was decreased in an inflammatory phase and increased above the homeostatic level during a recovery phase both in blood and colon lysates (Figure 24C-D), in line with previous reports. In line with this, Cxcl1 was decreased in blood and colon lysates derived from *Csf1r-cre;Ptger4*$^{fl/fl}$ mice at the recovery phase compared to *Ptger4*$^{fl/fl}$ (Figure 24E-F). Blocking endogenous COX activity by administrating indomethacin during colitis also showed shortened colon (Figure 24G) and reduced Cxcl1 levels in colon lysates (Figure 24H), which suggests that the increased Cxcl1 during the recovery phase is correlated with the increased PGE_2.

Next, I investigated the underlying signaling pathway of PGE_2 to the production of Cxcl1 in macrophages. First, I confirmed whether PGE_2 increases Cxcl1 through the

cAMP/PKA signaling pathway in macrophages, I treated adenylyl cyclase activator forskolin and PKA inhibitor. Forskolin did not increase Cxcl1 production and H89 increased Cxcl1 rather than decreased (Figure 25A). This result indicated that cAMP/PKA dependent pathway is not involved in production of Cxc1and blocking of PKA pathway could activate another pathway involved in Cxcl1 production. Because PGE_2 can increase expression of the Cxcl1 in colorectal cancer cells through the EGFR–MAPK cascade (40), I investigated whether PGE_2 up-regulates Cxcl1 through EGFR–MAPK pathway. I found that inhibitors for each MAPK and inhibitor of EGFR abrogated PGE_2-mediated Cxcl1 increases (Figure 25B-C). Taken together, these results showed that PGE_2 increased Cxcl1 production by activation EGFR and MAPKs signaling in activated macrophages.

Table 1. Disease active index of DSS induced colitis

Weight loss	score	Stool blood	score	Stool consistency	score
<1%	0	Absence	0	Formed and hard	0
1~5%	1			Formed but soft	1
5-10%	2	Presence	2	Loose stools	2
10-20%	3			Mild diarrhea	3
>20%	4	Gross bleeding	4	Gross diarrhea	4

Table 2. Primer sequences for QRT-PCR

Gene	Primers
Reg4	Forward: CTGGAATCCCAGGACAAAGAGTG Reverse: CTGGAGGCCTCCTCAATGTTTGC
Muc2	Forward: CAGTTTATTCCTGTGTGCCCAAGG Reverse: GGCTTCAGAATAATGTACTGCTGC
Bmi1	Forward: AATTAGTTCCAGGGCTTTTCAA Reverse: CTTCATCTGCAACCTCTCCTCTAT
Lgr5	Forward: GGGAGCGTTCACGGGCCTTC Reverse: GGTTGGCATCTAGGCGCAGGG
Lyz1	Forward: GAGACCGAAGCACCGACTATG Reverse: CGGTTTTGACATTGTGTTCGC
Lyz2	Forward: ATGGAATGGCTGGCTACTATGG Reverse: ACCAGTATCGGCTATTGATCTGA
Il-10	Forward: GGACAACATACTGCTAACCGAC Reverse: CCTGGGGCATCACTTCTACC
Cxcl1	Forward: TCCAGAGCTTGAAGGTGTTGCC Reverse: AACCAAGGGAGCTTCAGGGTCA
Arg1	Forward: GTCTGGCAGTTGGAAGCATCT Reverse: GCATCCACCCAAATGACACA
Mrc1	Forward: CATTCCCAGAGGAATTGCAT Reverse: AATGAAGATCACAAGCGC TGC
Ptger4 exon2	Forward: TGGTCATCTTACTCATCGCCAC Reverse: CCTTCACCACGTTTGGCTGAT

Table 3. List of used antibodies for Flow cytometry

Antibodies	Cat. No	Supplier
Anti-CD45	47-0451-82	e-bioscience
Anti-CD11b	48-0112-80	e-bioscience
Anti-Ly6G	551461	BD Pharmingen™
Anti-MHC Class II (I-A/I-E)	46-5321-80	e-bioscience
Anti -Ly6C	128017	Biolegend
Anti -CD64	558539	BD Pharmingen™
Anti FIZZ1/RETNL alpha	NBP2-29355	Novus biologics
Anti-Arginase 1	53-3697-82	e-bioscience
Anti-CD206	141703	biolegend
Anti-IL-10	11-7101-41	e-bioscience
Anti-EpCaM	118207	biolegend
Anti-EP4	101775	cayman chemical
Anti-rabbit IgG(H+L), secondary antibody,	R37116	thermofisher
anti- CD16/32	101301	biolegend
Anti-Ki67	12202	cell signaling

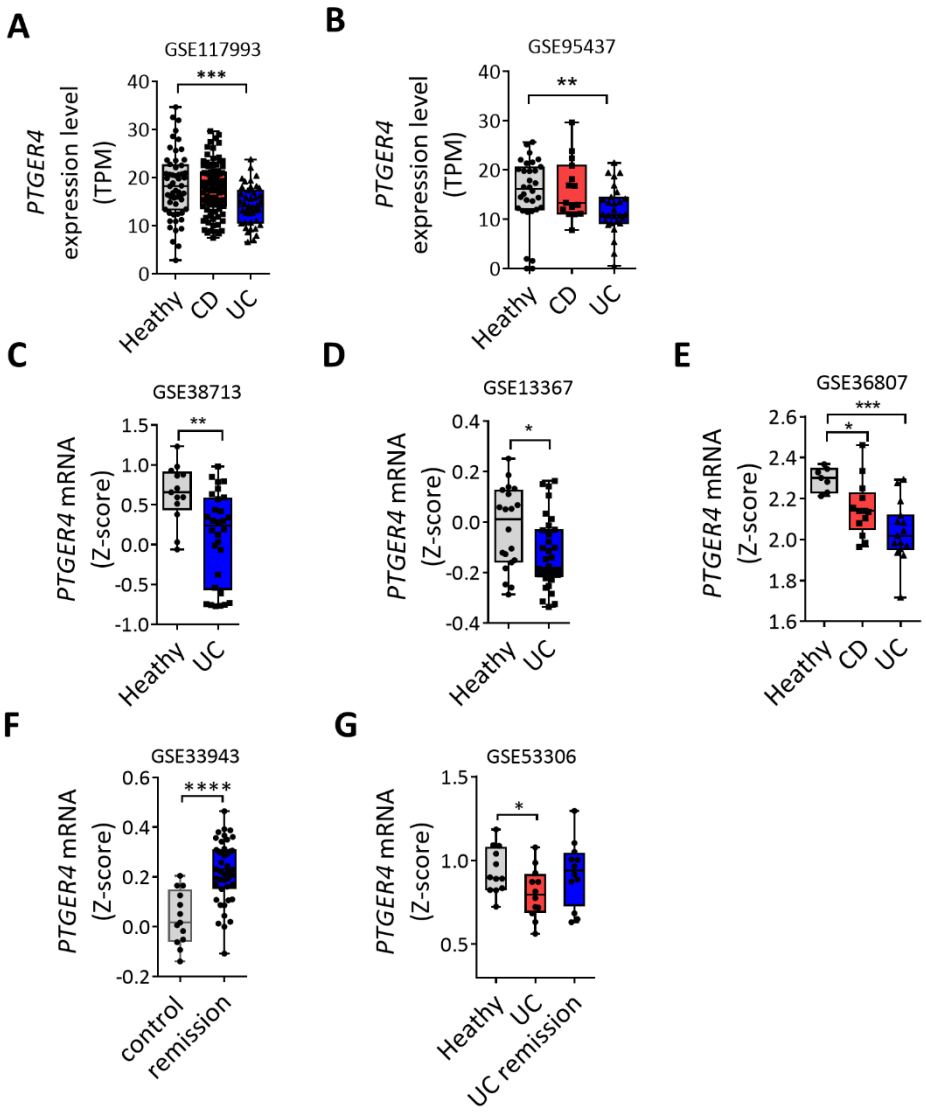

Figure 2. Expression of mRNA of PTGER4 was decreased in the human IBD patients

PTGER4 mRNA levels in the indicated IBD datasets. Box and whiskers graphs indicate the median and the 25th and 75th percentiles, with minimum and maximum values at the extremes of the whiskers. CD: crohn's disease, UC: ulcerative colitis. *$P < 0.05$, **$P < 0.01$, ***$P < 0.001$, ****$P < 0.0001$.

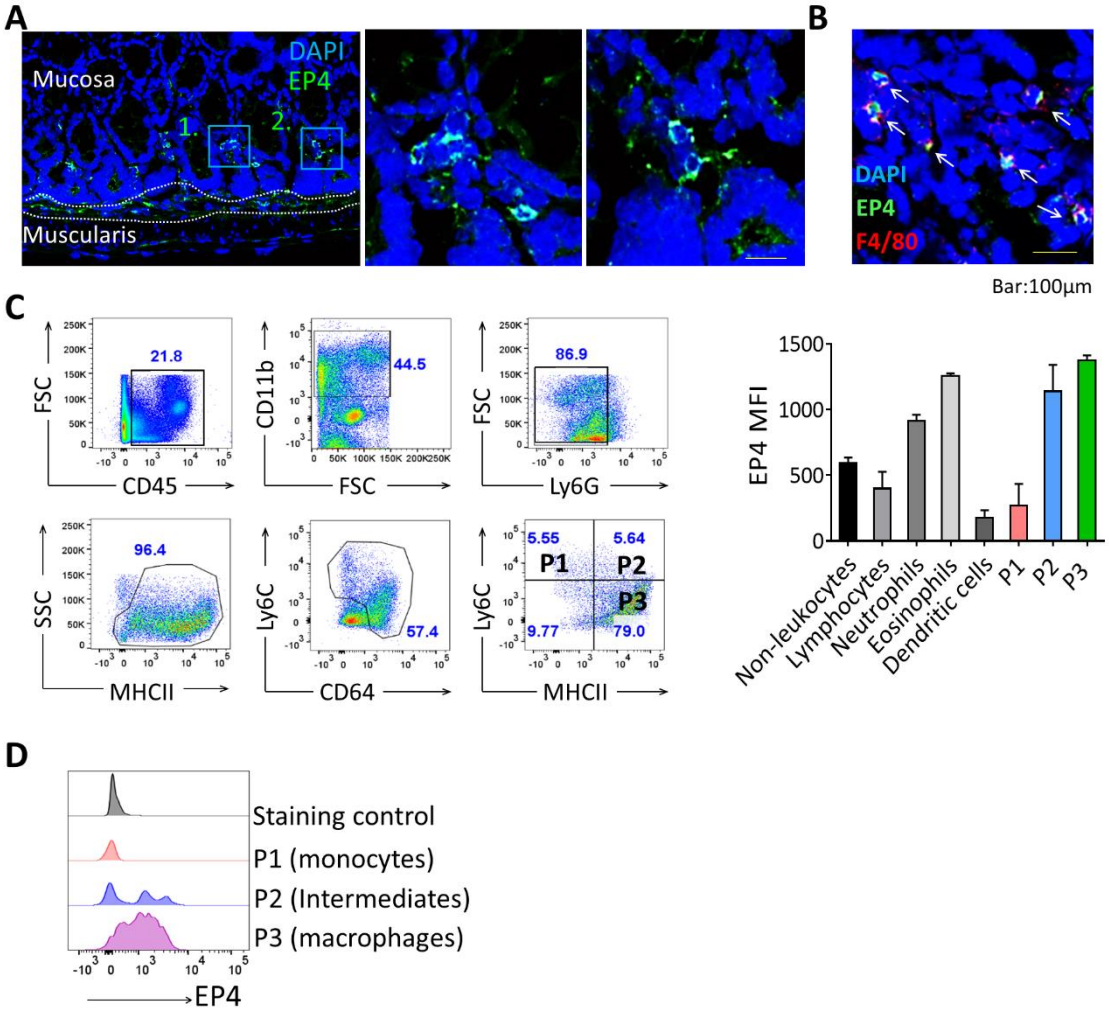

Figure 3. EP4 receptor expression in mouse colon

(A) Confocal images of colon sections of C57BL/6 mice stained for EP4 (green) and DAPI (blue). Scale bar = 100 μm. **(B)** Representative staining EP4 (green), F4/80 (Red) and DAPI (blue) on colon section. Arrows indicate double-positive cells. Scale bars = 100 μm. **(C)** Flow cytometry analysis of colonic lamina propria immune cells. Quantitative graph for the intensities of EP4 are shown in right. **(D)** Expression of EP4 protein in monocytes ($CD45^+CD11b^+Ly6G^-Ly6C^+MHCII^-$), intermediates ($CD45^+CD11b^+Ly6G^-Ly6C^+MHCII^+$) and macrophages ($CD45^+CD11b^+Ly6G^-Ly6C^+MHCII^+$) from colon lamina propria determined using flow cytometry.

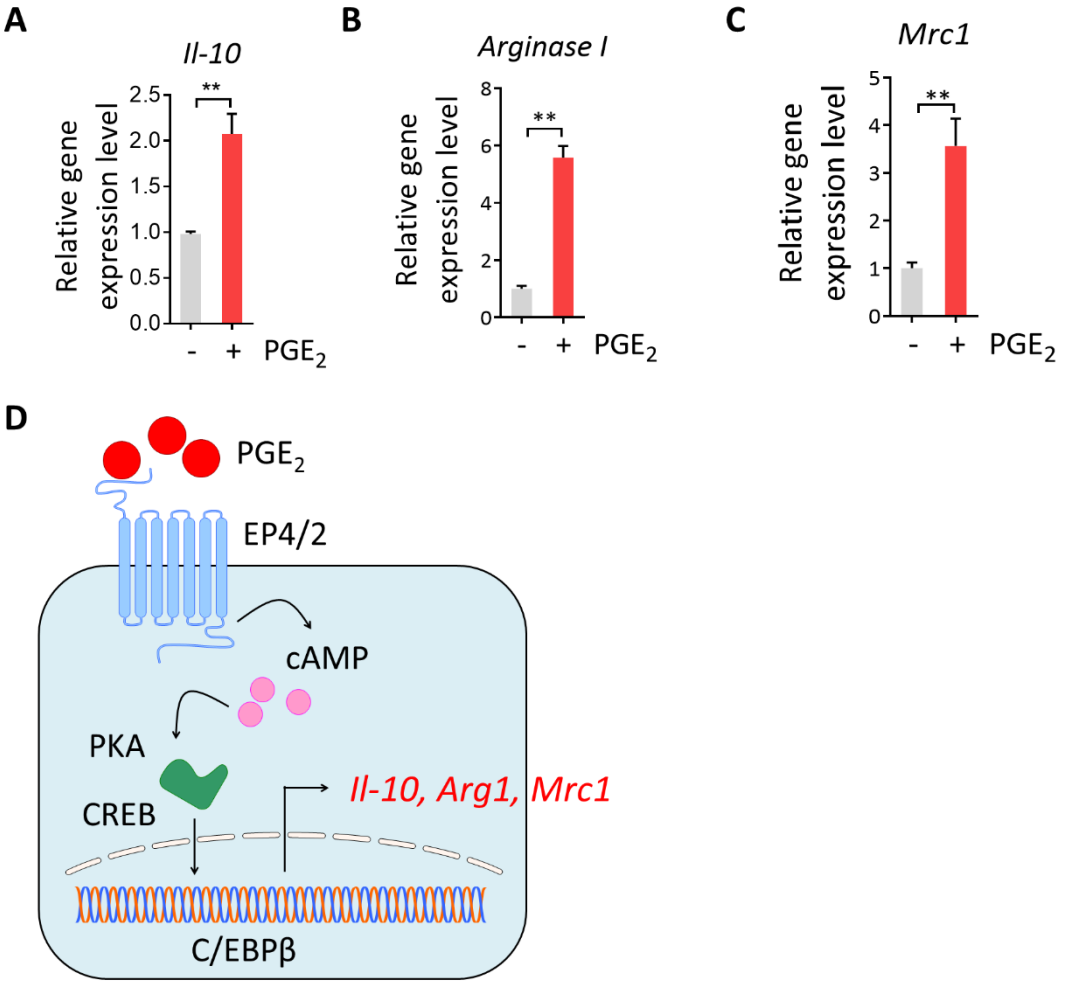

Figure 4. PGE_2 potentiates anti-inflammatory phenotype of macrophage through CREB-C/EBP-β cascade

Gene transcripts of *Il0* **(A)**, *Arg1* **(B)** and *Mrc1* **(C)** in bone marrow derived macrophages (BMDMs) determined using qPCR. BMDMs were treated with PGE_2 (10 μM) for 8 hours (n=3. $^{**}P < 0.01$). **(D)** Schematic figure shows the effect of endogenous PGE_2 on macrophage differentiation. Signaling by EP2 and EP4 is triggered by PGE_2 binding, and then adenylate cyclase is activated, leading to an increase in intracellular cyclic AMP (cAMP) levels, which in turn activates PKA. Activated PKA then causes phosphorylation of CREB. This leads to transcription of C/EBP-β which promotes *Arg1*, *Il10,* and *Mrc1* gene expression. Thus, PGE_2 promotes anti-inflammatory macrophage differentiation through the CREB/CEBP-β cascade.

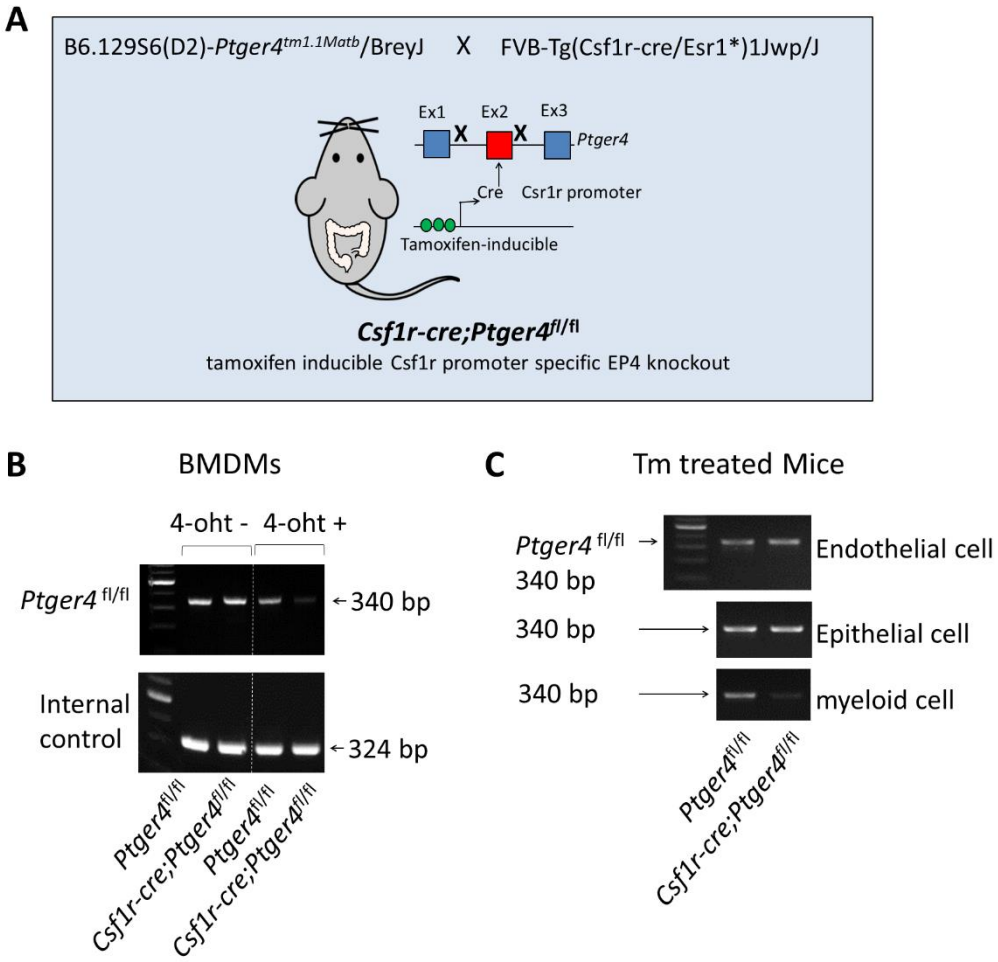

Figure 5. Generation of macrophage specific EP4 KO mice

(A) Generation of macrophage specific *Csf1r-cre;Ptger4*$^{fl/fl}$ mice. **(B)** PCR for the deleted allele of *Ptger4* (floxed, 340bp) of DNA from BMDMs of *Ptger4*$^{fl/fl}$ and *Csf1r-cre;Ptger4*$^{fl/fl}$ mice. To obtain an efficient deletion ex vivo, BMDMs were treated with 4-hydroxytamoxifen (4-oht) on the day4 and day6 during differentiation. **(C)** PCR for the deleted allele of *Ptger4* of DNA from sorted endothelial cell ($CD45^{-}CD31^{+}$), epithelial cells ($CD45^{-}EpCAM^{+}$) and myeloid cell ($CD45^{+}CD115^{+}$) of *Ptger4*$^{fl/fl}$ and *Csf1r-cre;Ptger4*$^{fl/fl}$ mice. Mice were exposed to tamoxifen (Tm) diet throughout experiment.

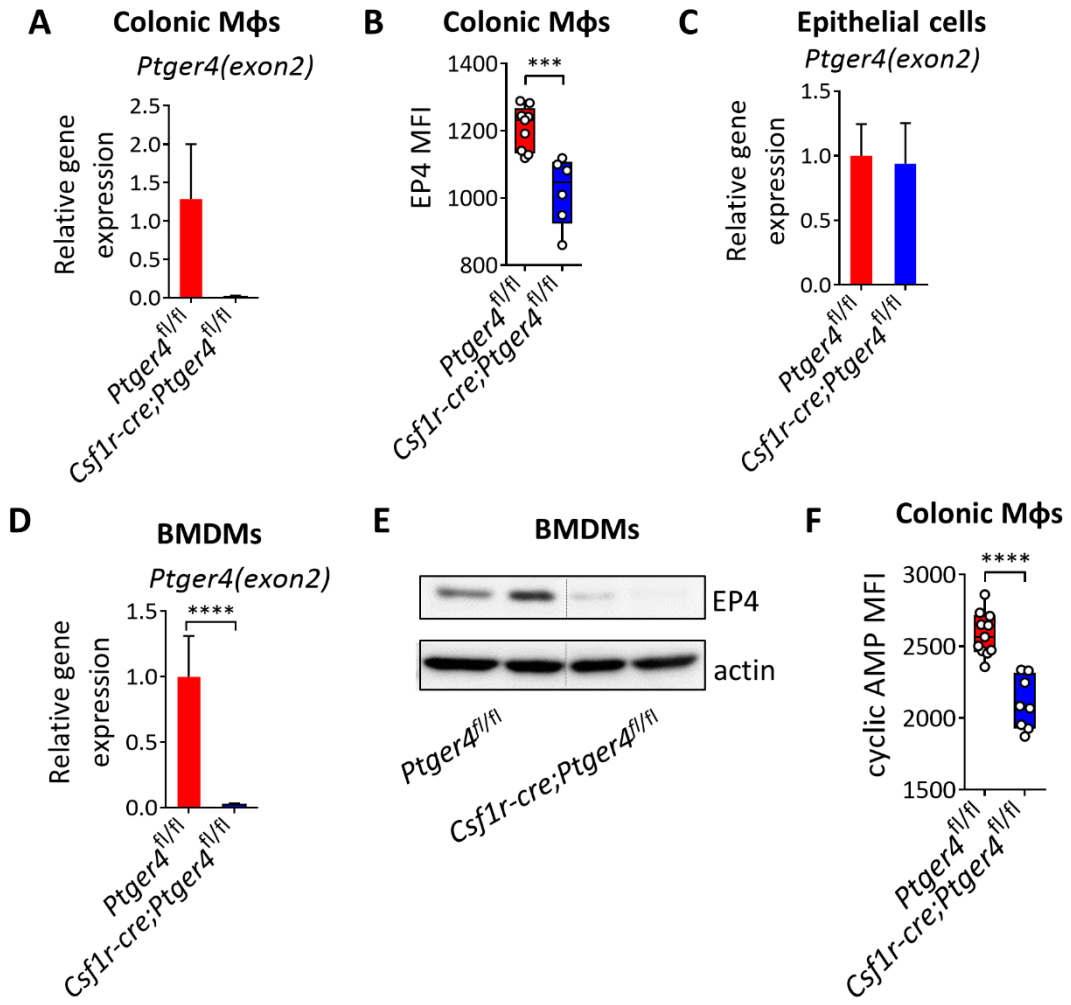

Figure 6. EP4 KO efficiencies of *Csf1r-cre;Ptger4*$^{fl/fl}$ mice

(A-C) Mice with macrophage deletion of EP4 were generated by exposure to tamoxifen diet throughout experiment. **(A)** Real time quantitative PCR analysis to determine mRNA of exon2 of *Ptger4* and **(B)** flow cytometry analysis to determine expression of EP4 protein in sorted $CD45^+CD11b^+Ly6G^-Ly6C^-MHCII^+$ macrophages of *Ptger4*$^{fl/fl}$ and *Csf1r-cre;Ptger4*$^{fl/fl}$ mice (***P<0.001). **(C)** Expression of mRNA of exon2 of *Ptger4* in epithelial cells from colon of *Ptger4*$^{fl/fl}$ and *Csf1r-cre;Ptger4*$^{fl/fl}$ mice. (**D-E**) BMDMs were treated with 4-oht on the day4 and day6 during differentiation. **(D)** Real time quantitative PCR analysis to determine mRNA and **(E)** western blot analysis to determine protein levels of EP4 in isolated BMDMs from *Ptger4*$^{fl/fl}$ and *Csf1r-cre;Ptger4*$^{fl/fl}$ mice

(****P < 0.0001). **(F)** Expression of cyclic AMP protein in macrophages ($CD45^+CD11b^+Ly6G^-Ly6C^+MHCII^-$) from colon lamina propria of *Ptger4*$^{fl/fl}$ and *Csf1r-cre;Ptger4*$^{fl/fl}$ mice determined using flow cytometry (n=11-8 per group. ****P < 0.0001).

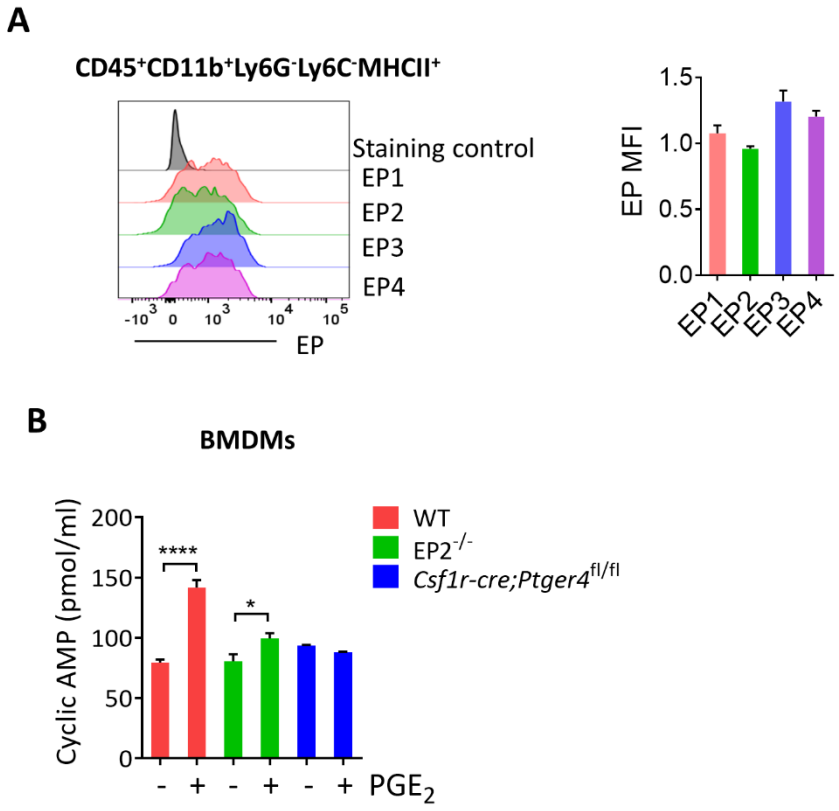

Figure 7. EP receptor expression in mouse colon

(A) EP 1-4 receptor protein content in $CD45^{+}CD11b^{+}Ly6G^{-}Ly6C^{-}MHCII^{+}$ macrophages from mice colon determined using flow cytometry. Quantitative graph for the intensities of EP receptor are shown in right. **(B)** Production of cyclic AMP levels in BMDMs of WT (*Ptger4*$^{fl/fl}$), EP2$^{-/-}$and *Csf1r-cre;Ptger4*$^{fl/fl}$ mice after 15min of PGE_2 treatment. BMDMs were treated with 4-oht on the day4 and day6 during differentiation (n=4. *$P < 0.05$, ****$P < 0.0001$).

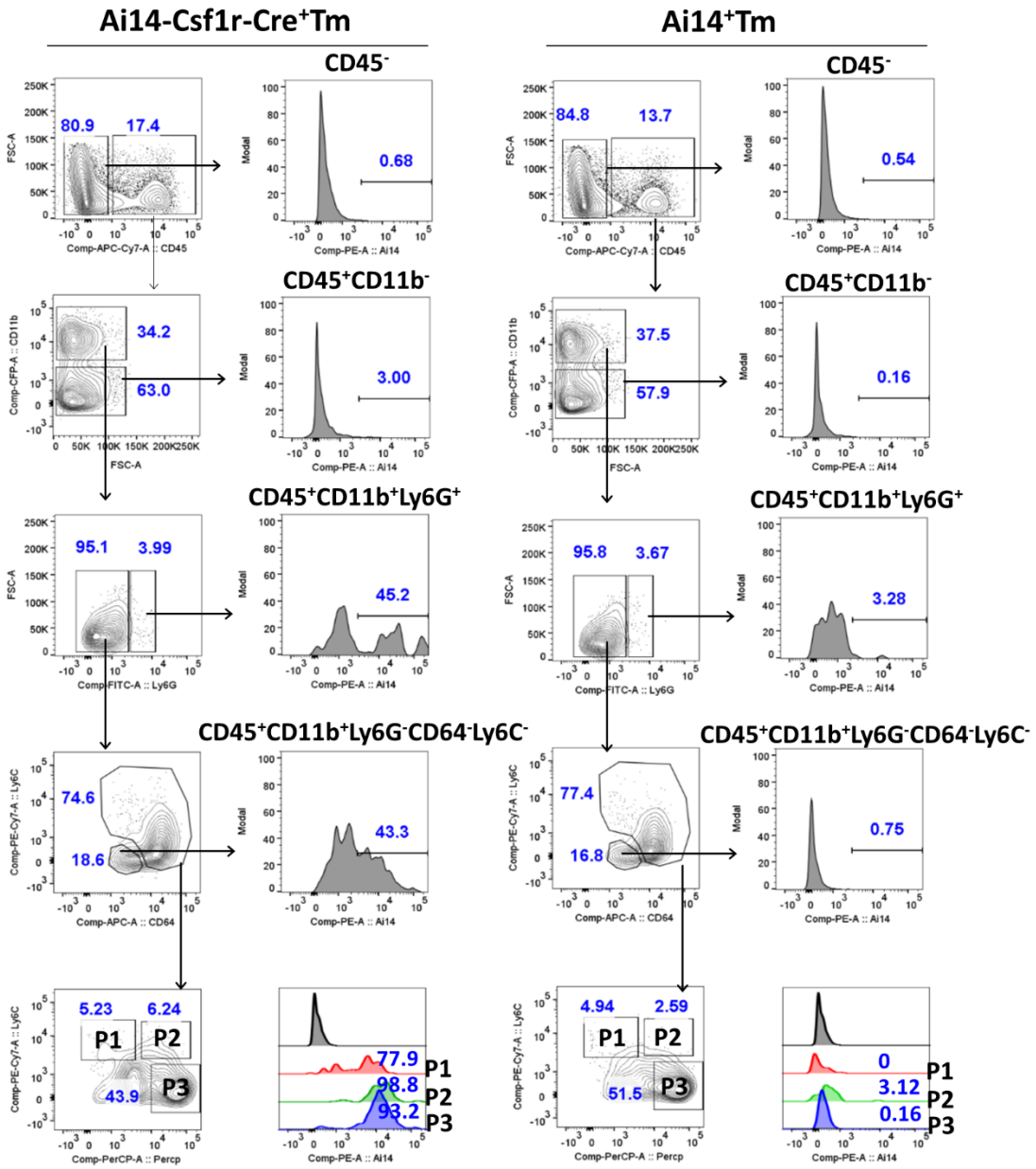

Figure 8. Distinct expression patterns of tdTomato in Csf1r^{+} cells of Csf1r-Ai14 mice

Representative flow cytometry plot of lamina propria cells in and Csf1r-Ai14 (left) and Ai14 mice (right) mice. Mice were administered tamoxifen (Tm) or corn oil by i.p. injection for five consecutive days.

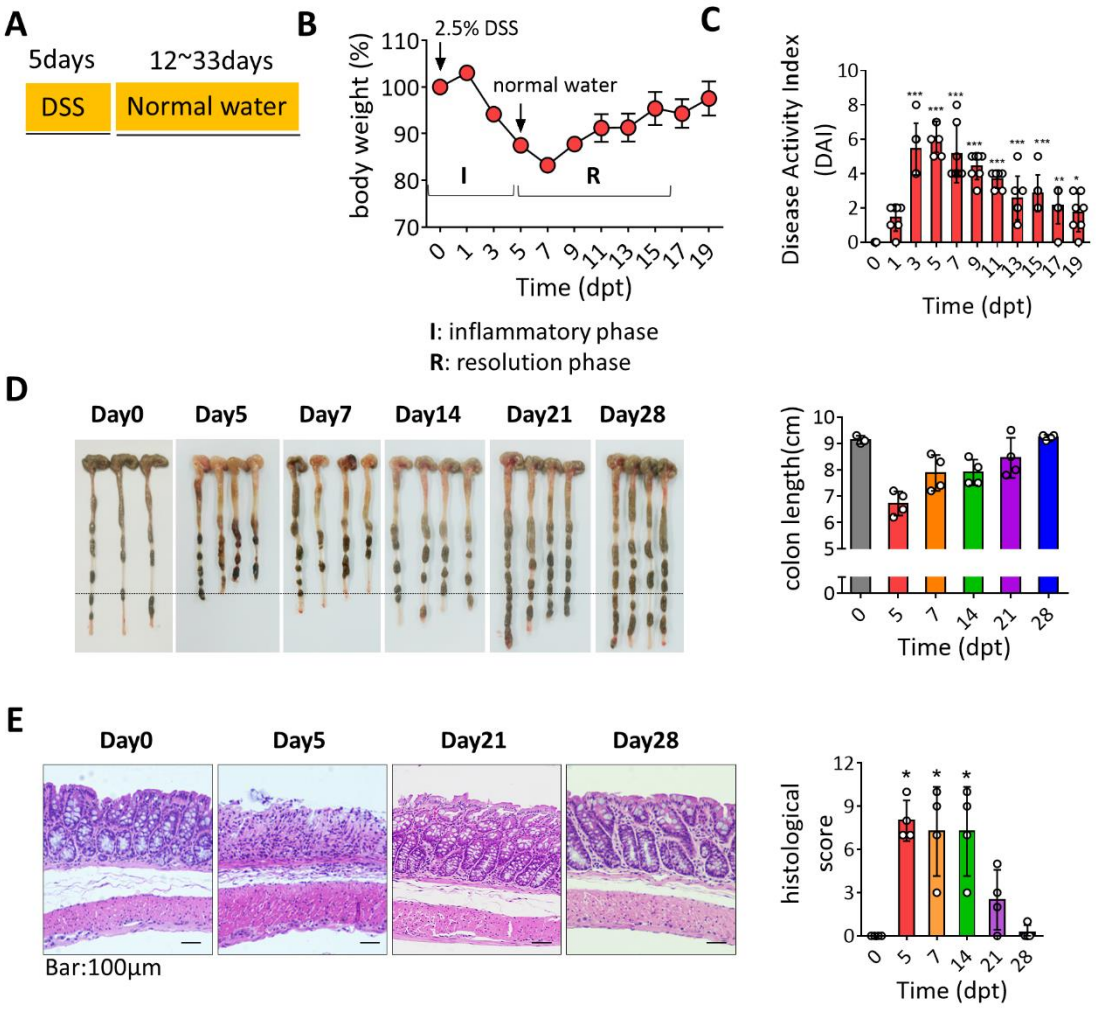

Figure 9. Characterization of DSS induced colitis model

(A) C57BL/6 mice were orally administered 2.5% DSS in drinking water for 5 days. **(B)** Percentage change in body weight. (n=7 per time point). **(C)** Disease activity index, a composite measure of weight loss, stool consistency and blood in stool (n=5-7 per time point, *$p < 0.05$, **$p < 0.01$, ***$P < 0.001$). **(D)** Left panel: representative images of mice colon at indicated time points. Right panel: Average of colon length with SEM at indicated time points. **(E)** Left panel: Representative images of hematoxylin and eosin staining of colon tissue from mice at indicated time points. Scale bars =100 μm. Right panel: Histological tissue damage and inflammation scoring at indicated time point (n=3 per time point, *$p < 0.05$).

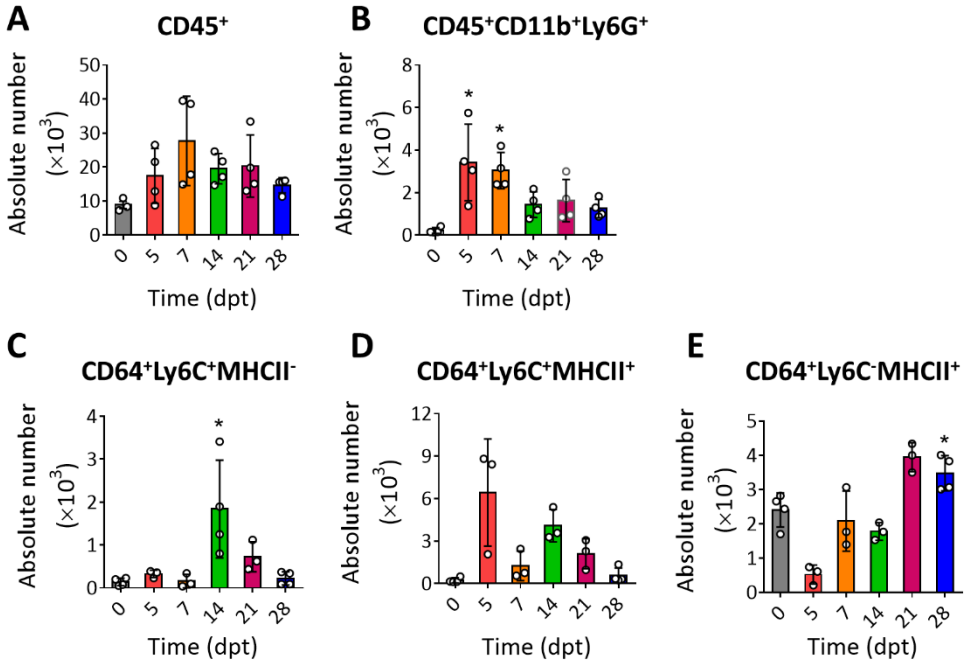

Figure 10. The numbers of immune cells in the colon during DSS-induced colitis

The number of $CD45^+$ leukocytes **(A)**, $CD45^+CD11b^+Ly6G^+$ neutrophils **(B)**, $CD64^+Ly6C^+MHCII^-$ monocyte **(C),** $CD64^+Ly6C^+MHCII^+$ intermediates **(D)** and $CD64^+Ly6C^-MHCII^+$ mature macrophages **(E)** in the colon lamina propria (n=3. $*P < 0.05$).

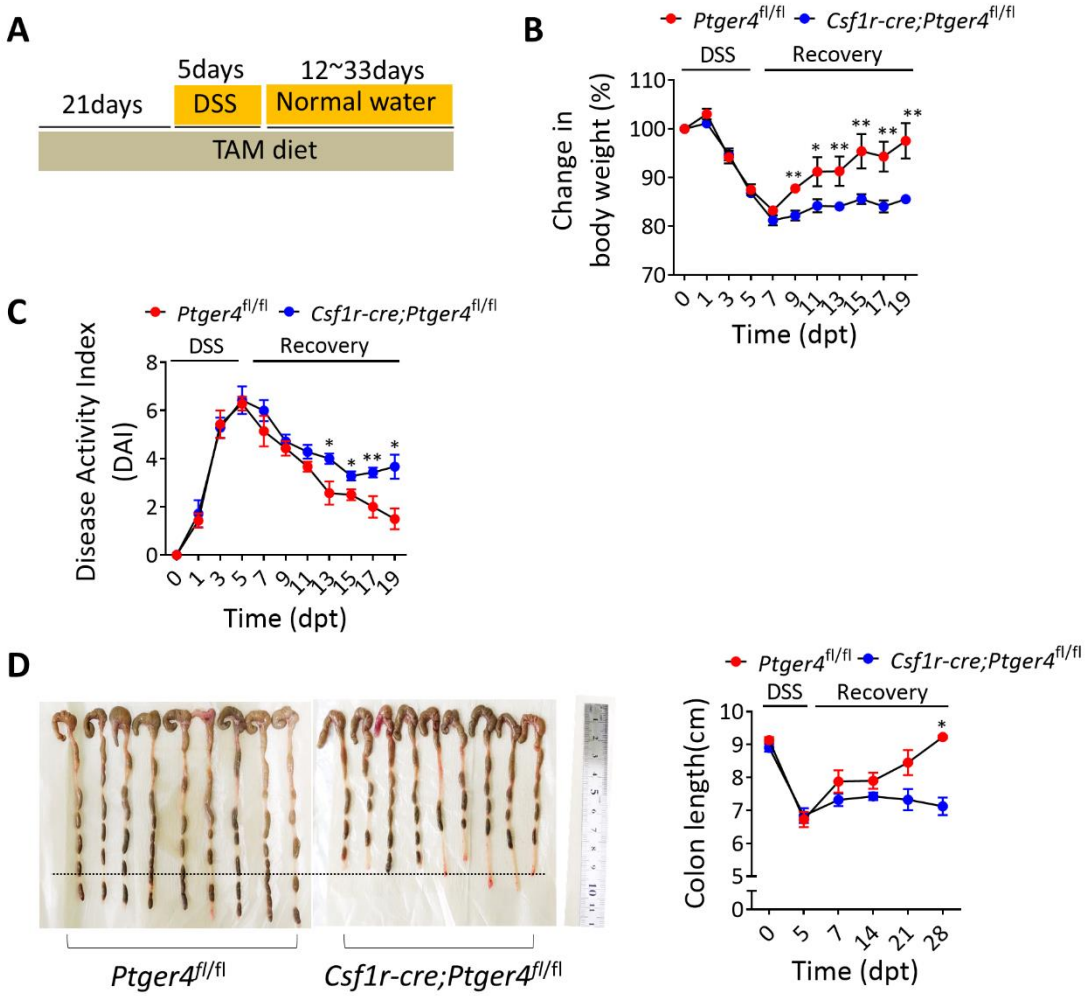

Figure 11. Csf1r- EP4-/- mice did not go through appropriate tissue regeneration

(A) *Ptger4*$^{fl/fl}$ and *Csf1r-cre;Ptger4*$^{fl/fl}$ mice were orally administered 2.5% DSS in drinking water for 5 days. Mice with macrophage deletion of EP4 were generated by exposure to tamoxifen diet throughout experiment. **(B)** Percentage change in body weight. (n=7 per time point, **P* < 0.05, ***P* < 0.01). **(C)** Disease activity index, a composite measure of weight loss, stool consistency and blood in stool (n=7 per time point, **p* < 0.05, ***P* < 0.01). **(D)** Left panel: representative images of *Ptger4*$^{fl/fl}$ and *Csf1r-cre;Ptger4*$^{fl/fl}$ mice colon on day 28. Right panel: Average of colon length with SEM at indicated time points (n=5-6 per time point, **P* < 0.05).

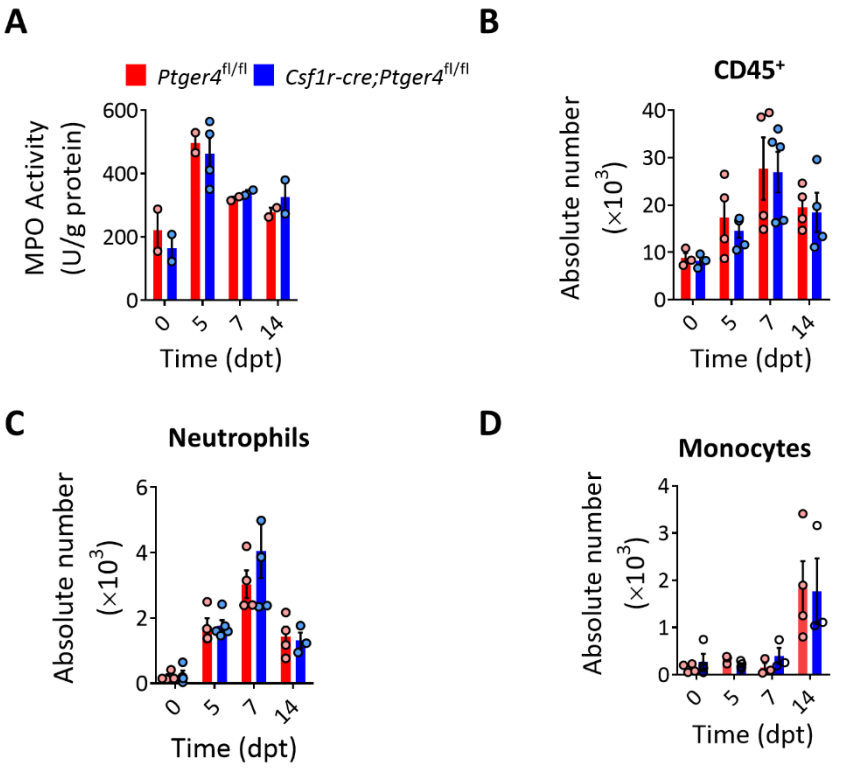

Figure 12. EP4 depletion of macrophages had no influence on the cellular proportion in lamina propria during colitis

Ptger4$^{fl/fl}$ and *Csf1r-cre;Ptger4*$^{fl/fl}$ mice were orally administered 2.5% DSS in drinking water for 5 days. Mice were exposed to tamoxifen diet throughout experiment. **(A)** MPO activity was measured in the colon lysate of *Ptger4*$^{fl/fl}$ and *Csf1r-cre;Ptger4*$^{fl/fl}$ mice at indicated time points. **(B-D)** The number of total leucocytes **(B)**, neutrophils **(C)** and monocytes **(D)** from *Ptger4*$^{fl/fl}$ and *Csf1r-cre;Ptger4*$^{fl/fl}$ mice colon were analyzed (n=2-4 per time point).

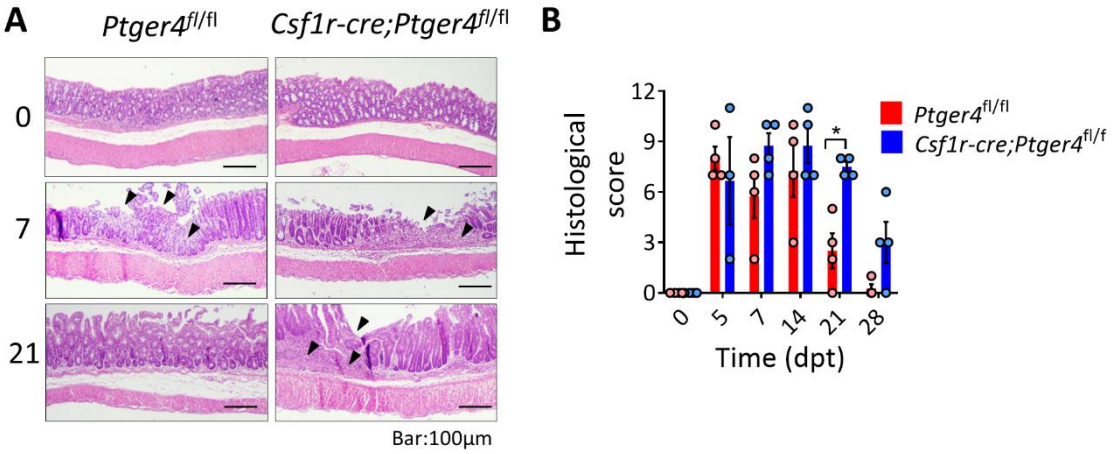

Figure 13. Deletion of EP4 in macrophages shows loss of mucosal regeneration

Ptger4$^{fl/fl}$ and *Csf1r-cre;Ptger4*$^{fl/fl}$ mice were orally administered 2.5% DSS in drinking water for 5 days. Mice were exposed to tamoxifen diet throughout experiment. **(A)** Representative images of hematoxylin and eosin staining of colon tissue from *Ptger4*$^{fl/fl}$ and *Csf1r-cre;Ptger4*$^{fl/fl}$ mice at indicated time point. Arrowhead: crypt loss and erosion. Scale bars = 100 μm. **(B)** Histological tissue damage and inflammation scoring at indicated time point (n=3-4 per time point, $*p < 0.05$).

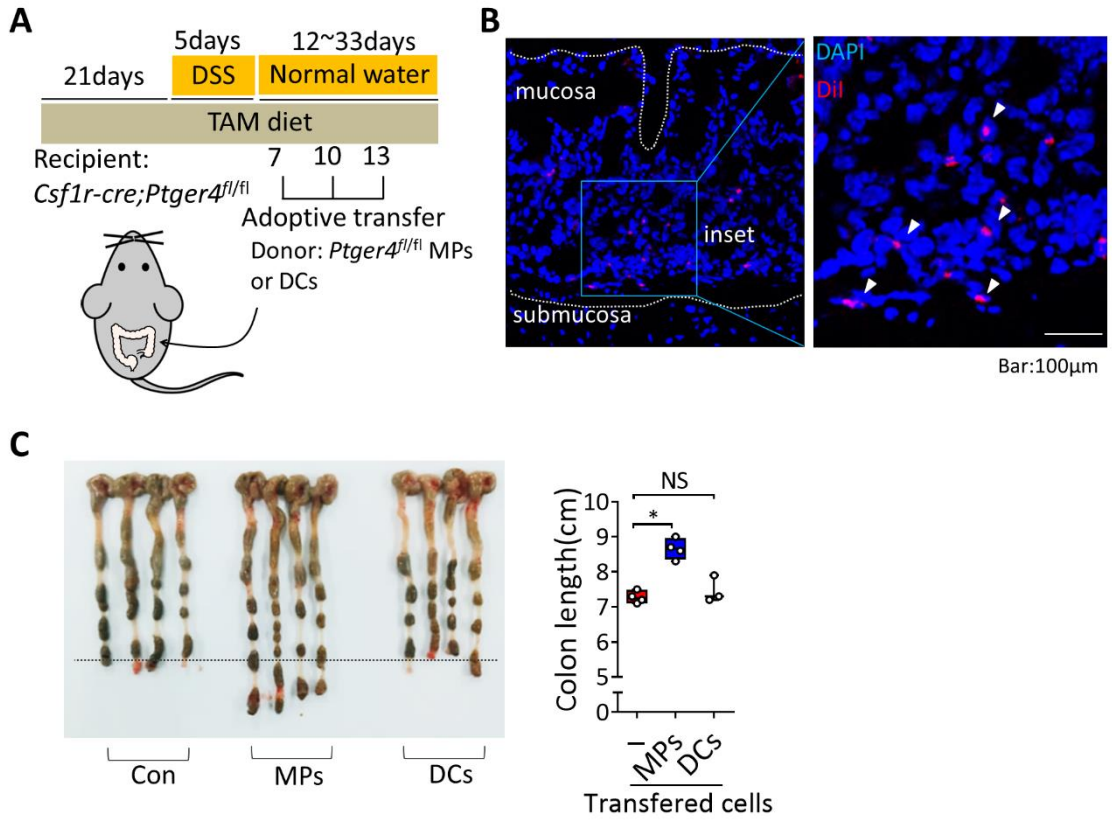

Figure 14. EP4 expressing macrophage is a major cellular source driving intestinal regeneration

(A) *Csf1r-cre;Ptger4*$^{fl/fl}$ mice were orally administered 2.5% DSS in drinking water for 5 days. Mice were exposed to tamoxifen diet throughout experiment. *Csf1r-cre;Ptger4*$^{fl/fl}$ mice were intraperitoneally injected (i.p.) with 2 × 10^6 macrophages (MPs) or dendritic cells (DCs) isolated from *Ptger4*$^{fl/fl}$ mice, as indicated (n = 3-4 per group). MPs were routinely > 95% F4/80+/CD11b+ cells and DCs were routinely > 40% $CD11c^+$ $CD11b^{int}$ MHC^{hi} cells. **(B)** Immunofluorescence staining for transferred cells (DiI, red) and nuclei (DAPI, blue) in colon tissues. Broken lines indicate the lamina propria boundary. Scale bars =100 μm. **(C)** Representative images of *Csf1r-cre;Ptger4*$^{fl/fl}$ mice colon on day 30. Right panel: Average of colon length with SEM (n=3-4 per group. *$P < 0.05$).

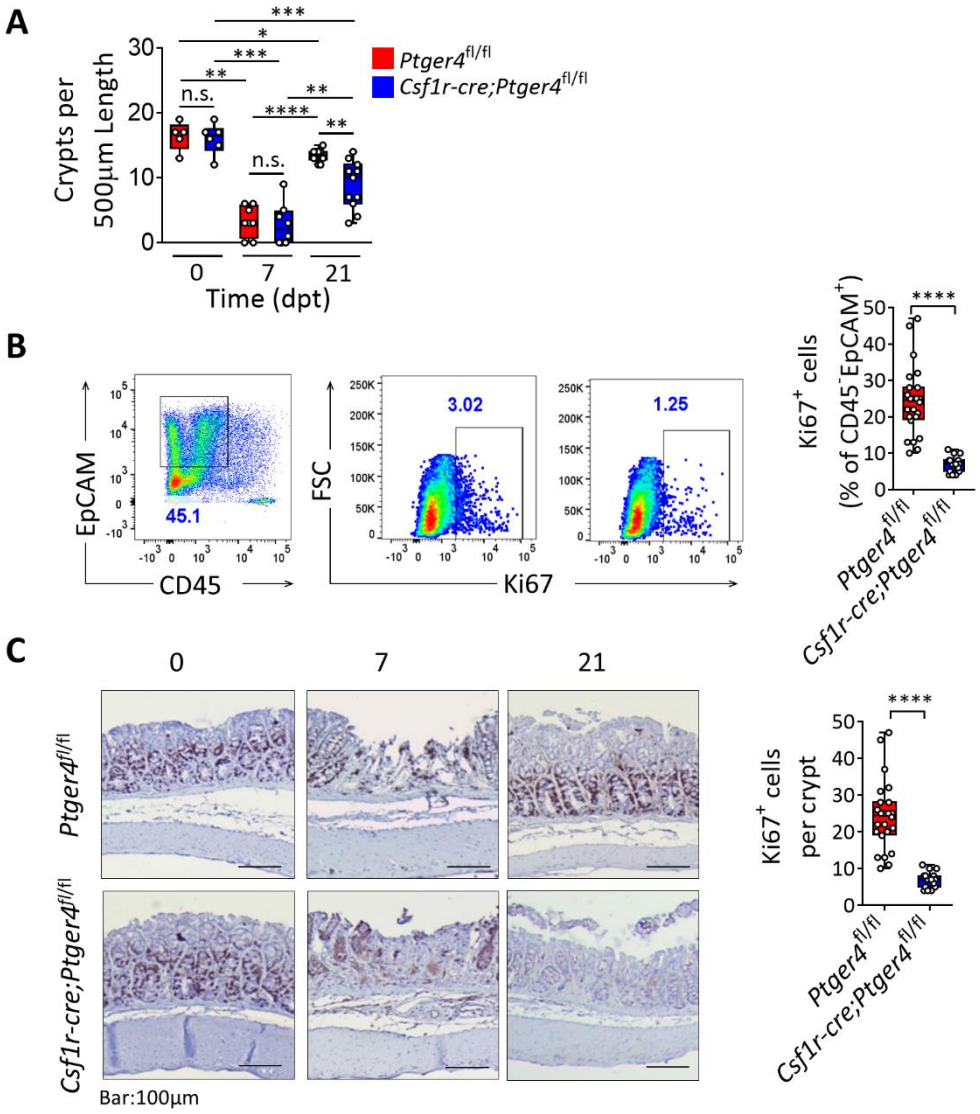

Figure 15. EP4 expressing macrophages induce regenerative responses of the damaged intestinal epithelium

Ptger4$^{fl/fl}$ and *Csf1r-cre;Ptger4*$^{fl/fl}$ mice were orally administered 2.5% DSS in drinking water for 5 days. Mice were exposed to tamoxifen diet throughout experiment. **(A)** The number of crypts in 500 µm length of colon were measured using Image (n=7 per time point, **P* < 0.05, ***P* < 0.01, ****P* < 0.001, *****P* < 0.0001). **(B)** Ki67^{+} epithelial cell isolated from *Ptger4*$^{fl/fl}$ and *Csf1r-cre;Ptger4*$^{fl/fl}$ mice on day 28 determined using flow cytometry. Gating of CD45^{-}EpCAM^{+} epithelial cells and quantitative graph for the

number of Ki67^{+} cells are shown in right. (n=15-20 per group, ****$P < 0.0001$) **(C)** Left panel: Representative images of Ki67 staining in the colon of *Ptger4*$^{fl/fl}$ and *Csf1r-cre;Ptger4*$^{fl/fl}$ mice from different times during DSS-induced colitis are shown. Scale bars = 100 μm. Right panel: The number of Ki67^{+} cells/colon crypt was quantified on day 21 (n=15-20. ****$P < 0.0001$).

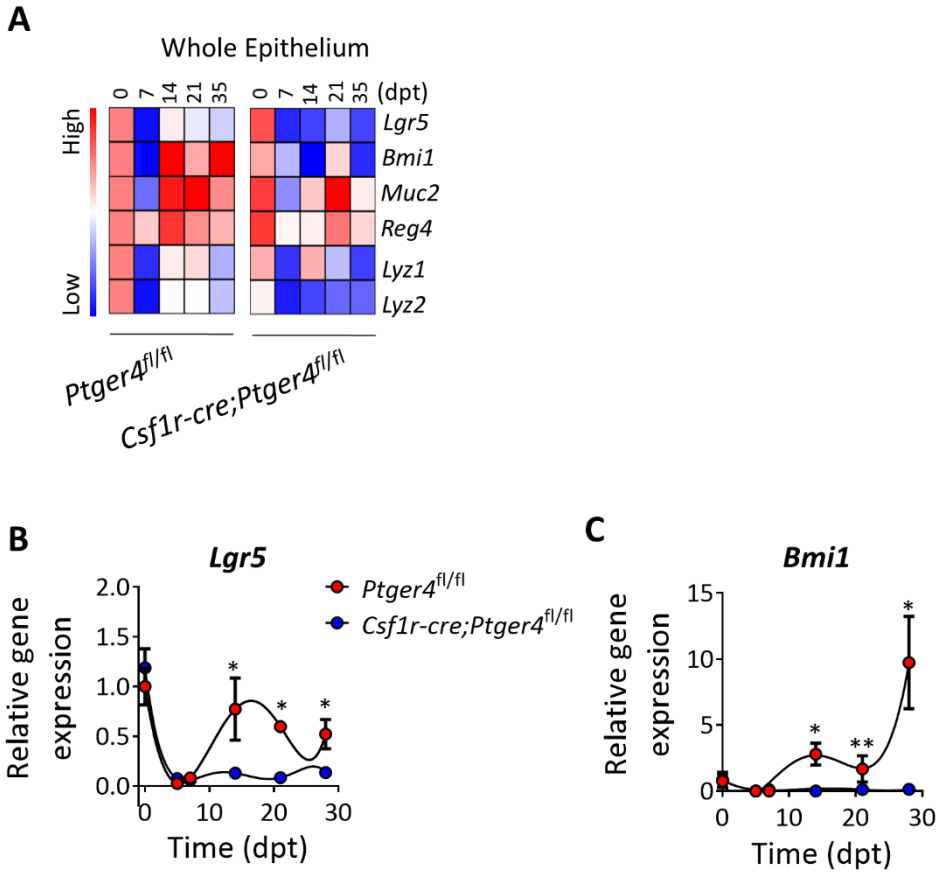

Figure 16. Expression of epithelial proliferation related genes is reduced in epithelium from *Csf1r-cre;Ptger4*$^{fl/fl}$ mice

(A) Heat maps representing genes (labels to the right of plots) with relative gene expression in whole colon epithelium of *Ptger4*$^{fl/fl}$ and *Csf1r-cre;Ptger4*$^{fl/fl}$ mice using quantitative real-time PCR (qPCR). Warm color (red) denotes an increase of gene expression whereas cold color (blue) indicates a decrease compared to average level of gene expression in naïve *Ptger4*$^{fl/fl}$. Gene expression of Lgr5 **(B)** and Bmi1 **(C)** at indicated time point (n=3 per time point, $*P < 0.05$, $**P < 0.01$).

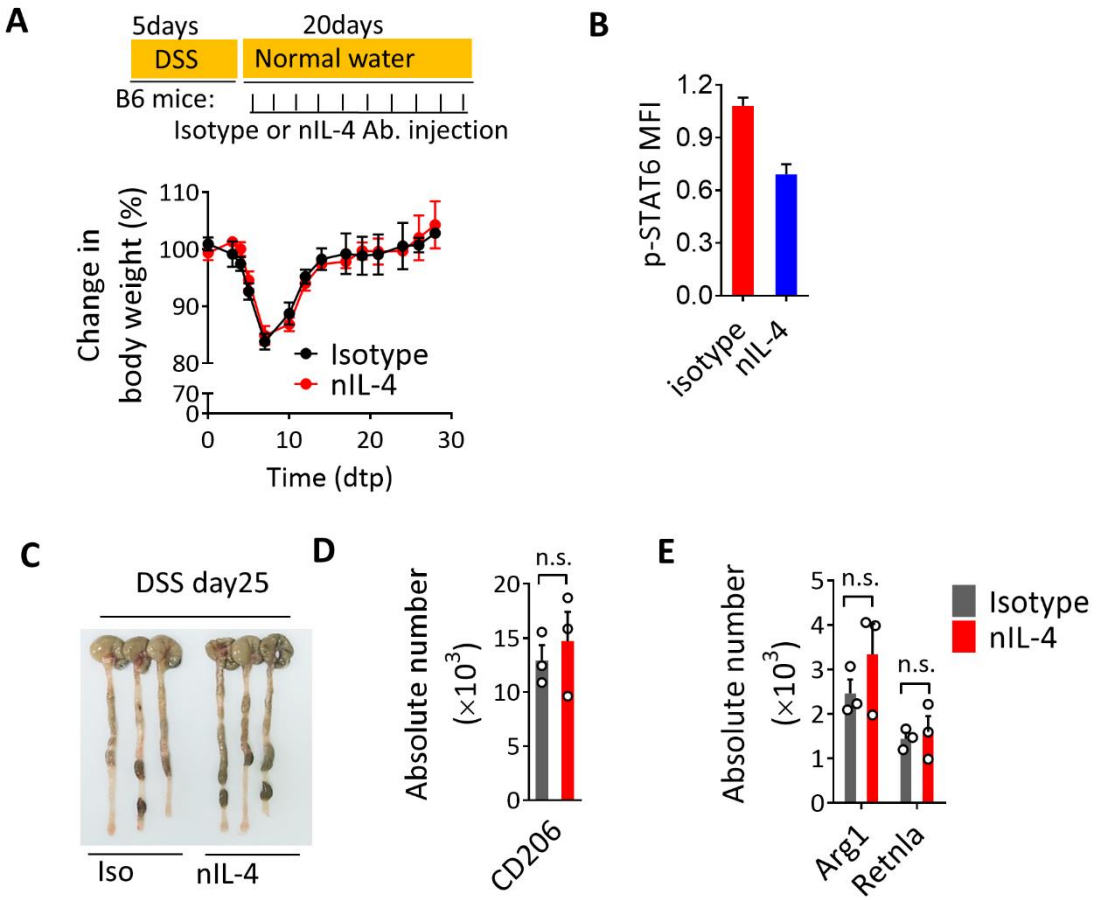

Figure 17. IL-4 is not required for intestinal wound healing

(A) C57BL/6 mice were orally administered 2.5% DSS in drinking water for 5 days. IL-4 neutralizing antibody (nIL-4 Ab) or corresponding isotype Abs (25 μg per mouse) were injected i.p. three times a week throughout the whole recovery period. Percentage change in body weight. (n=3 per time point). **(B)** Quantitative graph shows the intensities of p-STAT6 in $CD45^+CD11b^+Ly6G^-Ly6C^-MHCII^+$ macrophages from mice colon. **(C)** Representative images of colon of mice treated with nIL-4 Ab or control-IgG on day 25. The number of $CD206^+$ **(D)**, $Arg1^+$ and $Retnla^+$ **(E)** macrophages from colon of nIL-4 Ab or control-IgG injected mice were analyzed (n=3 per group).

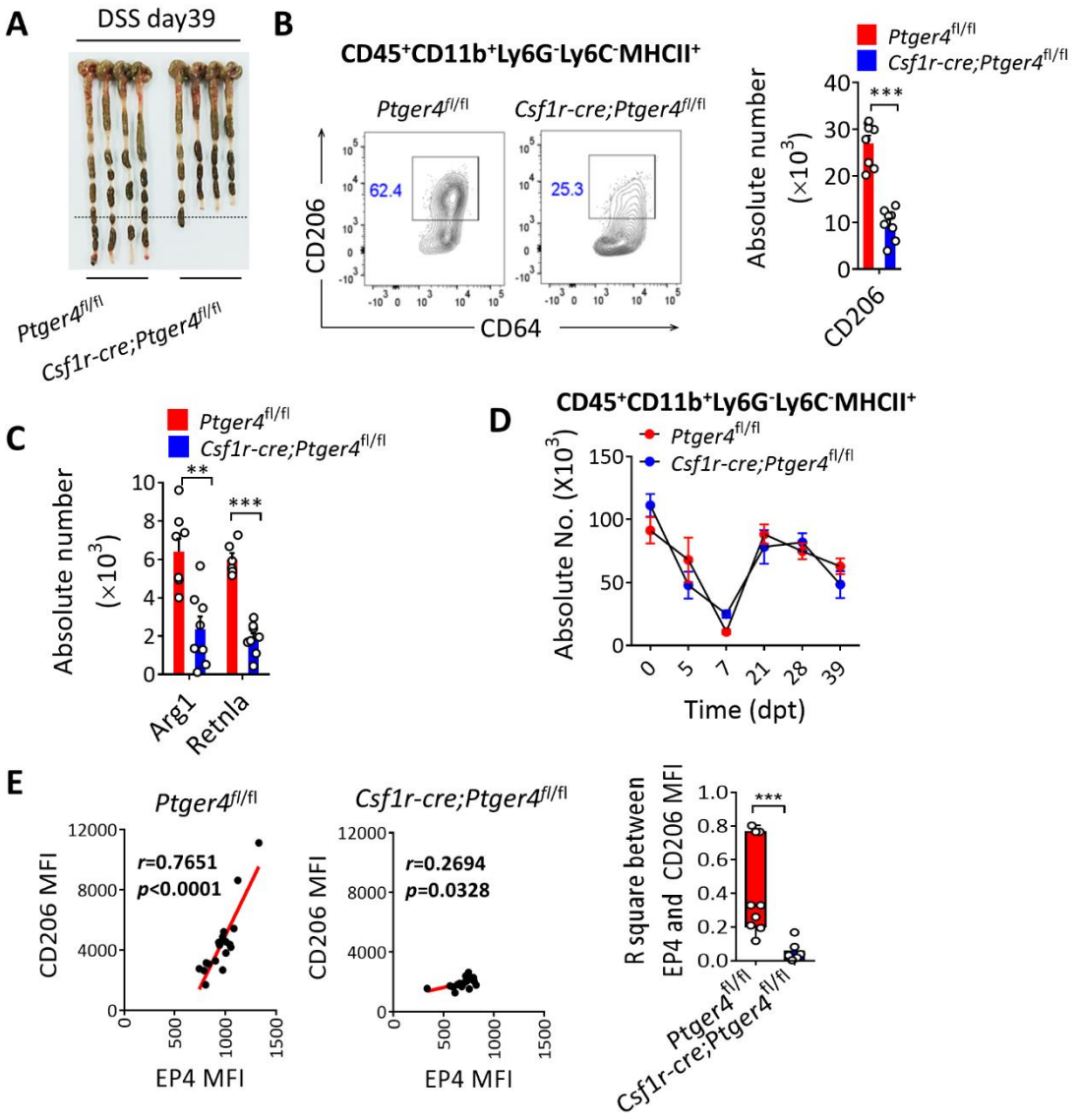

Figure 18. Macrophage EP4 signaling promotes the wound healing function of colonic macrophages

(A-C) *Ptger4*$^{fl/fl}$ and *Csf1r-cre;Ptger4*$^{fl/fl}$ mice on day 39 after induction with 2.5% DSS in the drinking water. Mice were exposed to tamoxifen diet throughout experiment**. (A)** representative images of *Ptger4*$^{fl/fl}$ and *Csf1r-cre;Ptger4*$^{fl/fl}$ mice colon. The number of CD206^{+} **(B)**, Arg1^{+} and Retnla^{+}**(C)** macrophages (CD45^{+}CD11b^{+}Ly6G^{-}Ly6C^{-}MHCII^{+}) from *Ptger4*$^{fl/fl}$ and *Csf1r-cre;Ptger4*$^{fl/fl}$ mice colon was analyzed (n=8 per group, $^{**}p < 0.01$, $^{***}p < 0.001$). **(D)** The number of CD64^{+}Ly6C^{-}MHCII^{+} mature macrophages in

colon from *Ptger4*$^{fl/fl}$ and *Csf1r-cre;Ptger4*$^{fl/fl}$ mice at indicated time points (n=3-4 per time points). **(E)** Correlation plot between relative mean fluorescent intensity (MFI) of EP4 and CD206 of $CD45^{+}CD11b^{+}Ly6G^{-}Ly6C^{-}MHCII^{+}$macrophages from *Ptger4*$^{fl/fl}$ and *Csf1r-cre;Ptger4*$^{fl/fl}$ mice colon. Quantitative graph for the R square of EP4 and CD206 are shown in right.

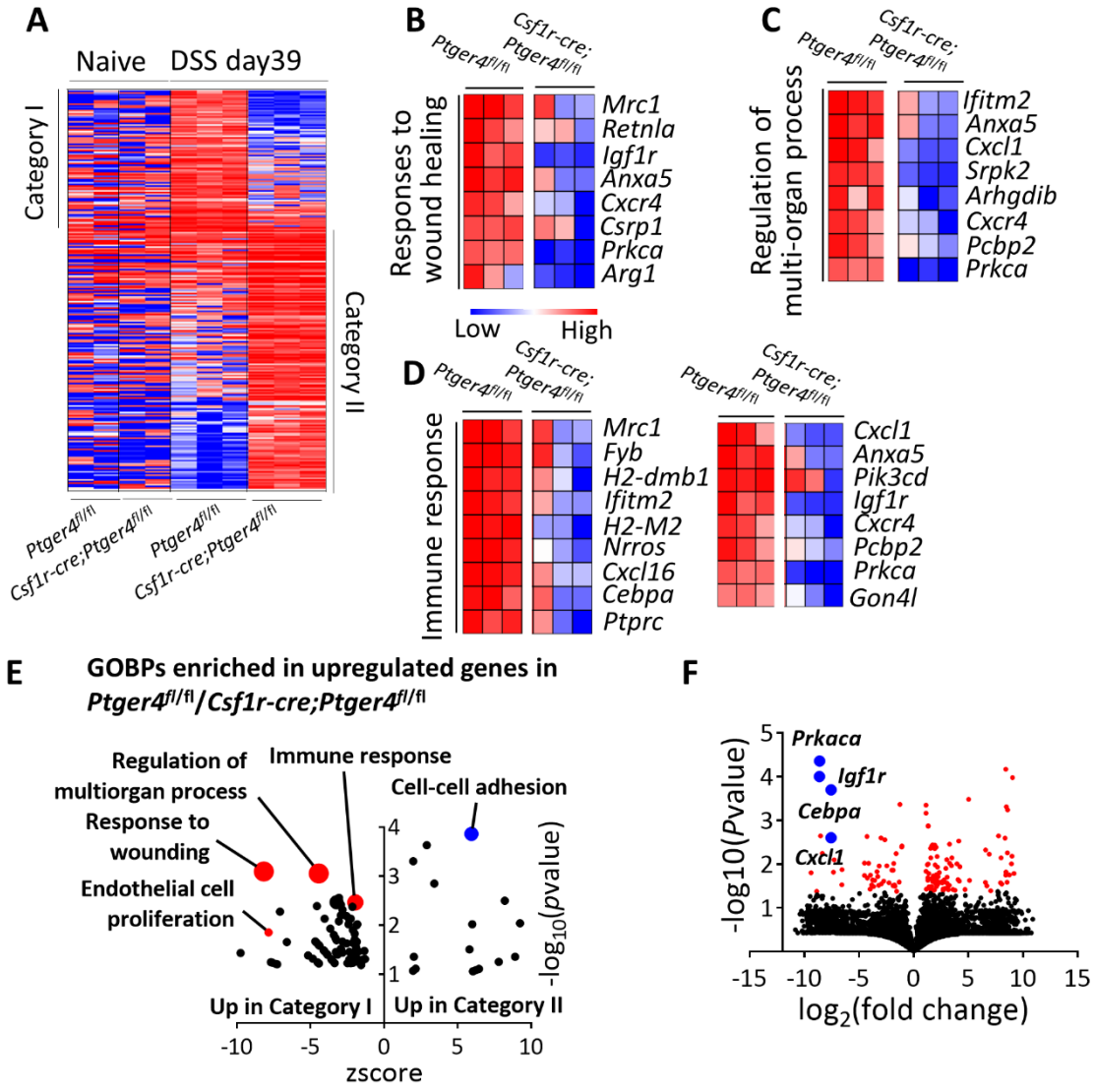

Figure 19. RNAseq of colonic macrophages reveals EP4 signaling in macrophages is require for wound healing function

(A-F) Genome-wide transcriptional profiles of colonic macrophages of *Ptger4*$^{fl/fl}$ and *Csf1r-cre;Ptger4*$^{fl/fl}$ mice from different times during DSS-induced colitis. **(A)** upregulated gene set in *Ptger4*$^{fl/fl}$ (Category I) and *Csf1r-cre;Ptger4*$^{fl/fl}$ (Category II). Heat maps representing genes (labels to the right of plots) clustered in Gene Ontology Biological Process (GOBP) responses to wound healing **(B)**, regulation of multi-organ process **(C)** and immune response **(D)** (labels to the left of plots) with scaled $\log_2$

fluorescence intensity. Warm color (red) denotes an increase of gene expression whereas cold color (blue) indicates a decrease compared to average level of gene expression in naïve macrophages. **(E)** GO analysis of *Ptger4*$^{fl/fl}$ up-regulated genes in colonic macrophages. **(F)** Volcano plot of the RNA-seq data.

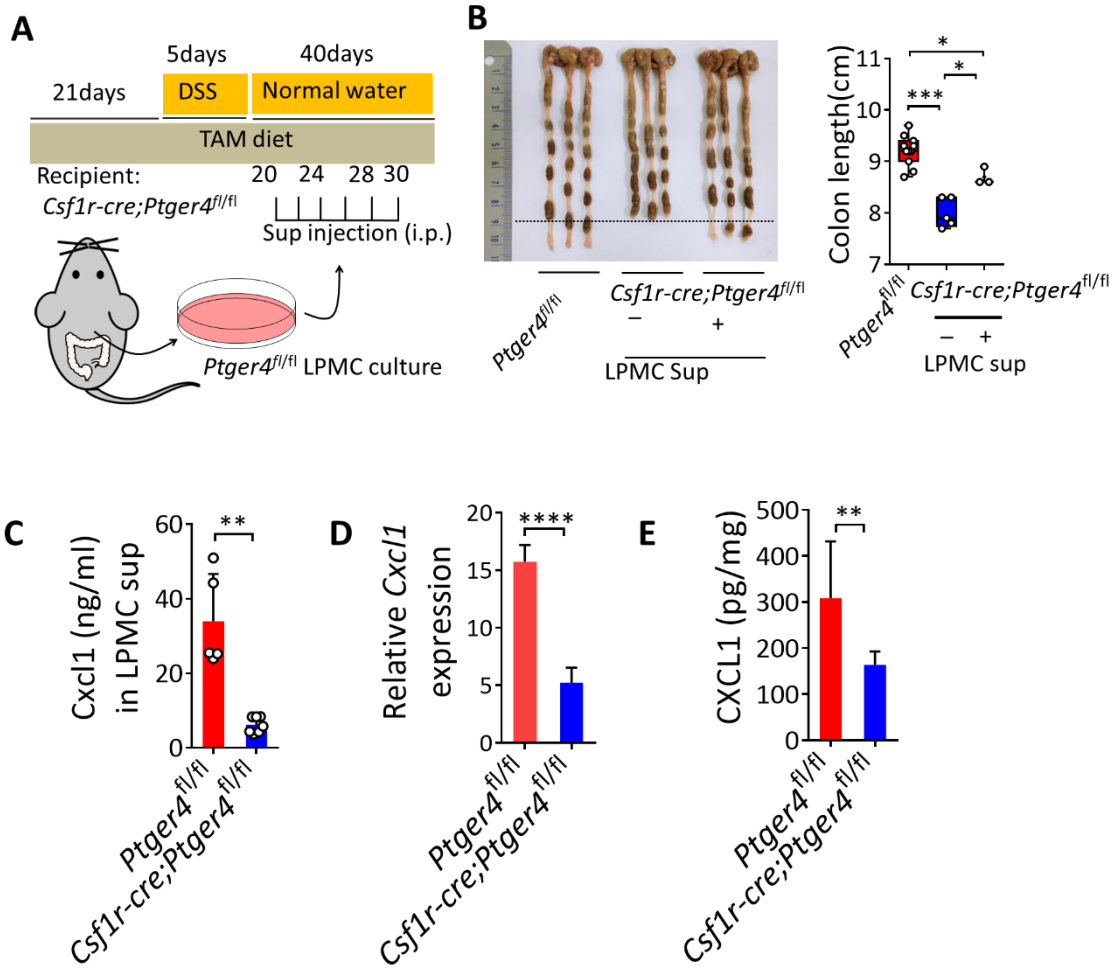

Figure 20. Cxcl1 production is reduced in colon lamina propria mononuclear cells (LPMCs) from *Csf1r-cre;Ptger4*$^{fl/fl}$ mice

(A) *Ptger4*$^{fl/fl}$ and *Csf1r-cre;Ptger4*$^{fl/fl}$ mice were orally administered 2.5% DSS in drinking water for 5 days. Mice were exposed to tamoxifen diet throughout experiment. *Csf1r-cre;Ptger4*$^{fl/fl}$ mice were injected with the supernatant of WT lamina propria mononuclear cells (LPMC) total six times. **(B)** Representative images of *Ptger4*$^{fl/fl}$ and *Csf1r-cre;Ptger4*$^{fl/fl}$ mice colon with or without LPMC culture supernatant on day 40. Right panel: Average of colon length with SEM (n=3-9 per group. *$P < 0.05$, ***$P < 0.001$). **(C)** Cxcl1 levels in LPMC culture supernatant obtained from *Ptger4*$^{fl/fl}$ and *Csf1r-cre;Ptger4*$^{fl/fl}$ mice (n=5-6. **$P < 0.01$). Relative Cxcl1 gene expression **(D)** and Cxcl1

levels **(E)** in whole colon of *Ptger4*$^{fl/fl}$ and *Csf1r-cre;Ptger4*$^{fl/fl}$ mice (n=5-6. $^{**}P < 0.01$, $^{****}P < 0.00001$)

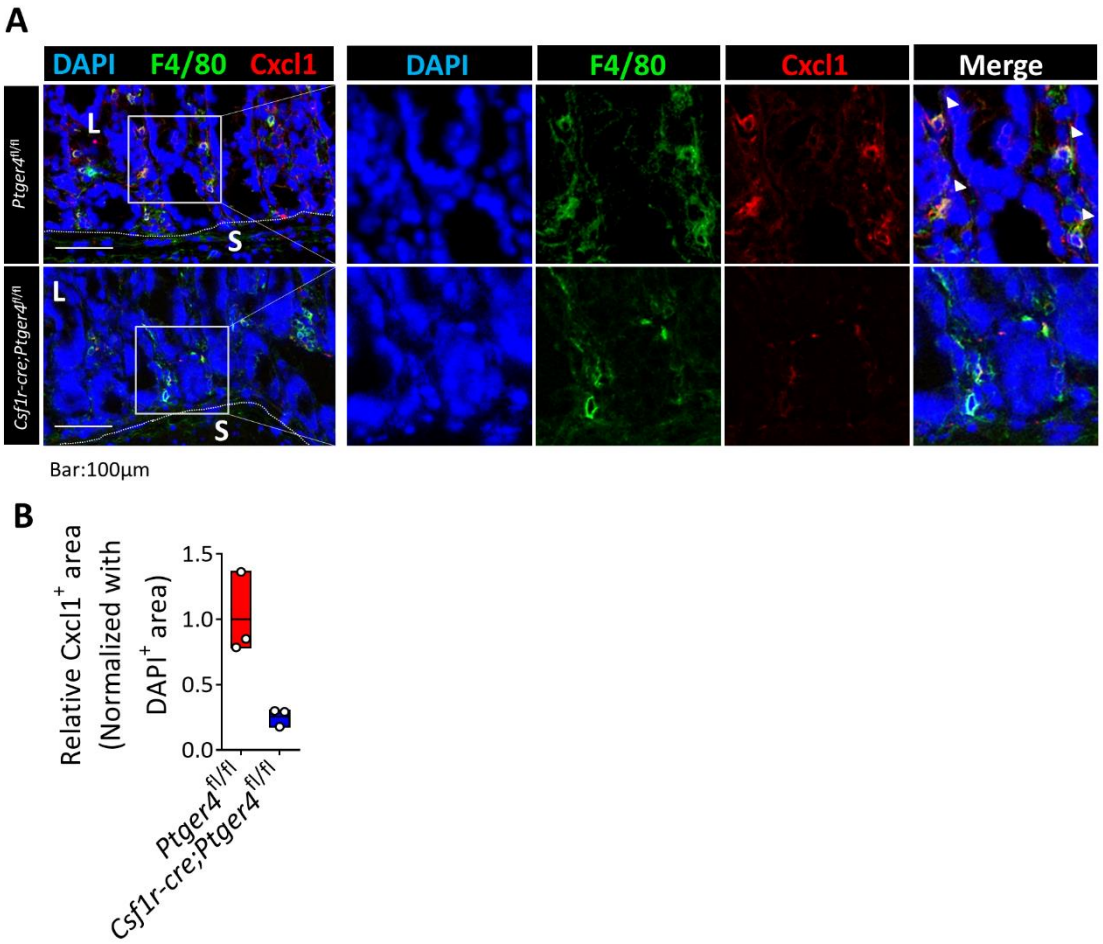

Figure 21. Expression of Cxcl1 is reduced in colon of *Csf1r-cre;Ptger4*$^{fl/fl}$ mice

(A) Confocal images of colon sections of *Ptger4*$^{fl/fl}$ and *Csf1r-cre;Ptger4*$^{fl/fl}$ mice stained for F4/80 (green), Cxcl1 (Red) and DAPI (blue). Arrows indicate double-positive cells. Scale bar, 100 μm. **(B)** Relative Cxcl1 intensities normalized by DAPI intensity (n=3.).

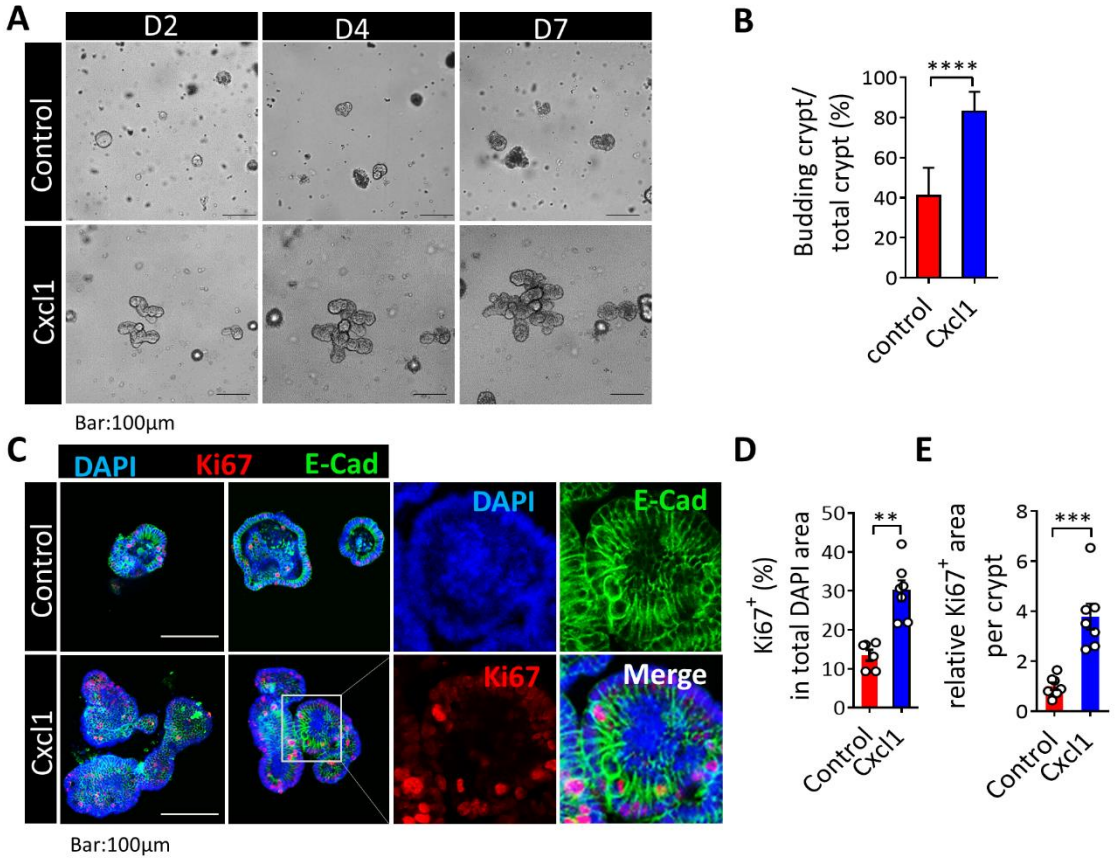

Figure 22. Cxcl1 is necessary for the intestinal epithelial regeneration

(A) The intestinal crypt organoids were cultured with differentiation medium containing recombinant Cxcl1 (10ng/ml). **(B)** Quantitative statistics of the number of budding crypts (D7) after incubation with recombinant Cxcl1 were compiled (n=10-11. ****$P < 0.001$). Scale bar, 100 μm. **(C)** Confocal images of intestinal crypt organoids stained for E-Cadherin (green), Ki67 (Red) and DAPI (blue). Scale bar, 100 μm. Relative Ki67 intensities normalized by DAPI intensity **(D)** and per crypt **(E)** (n=6. **$P < 0.01$,***$P < 0.001$).

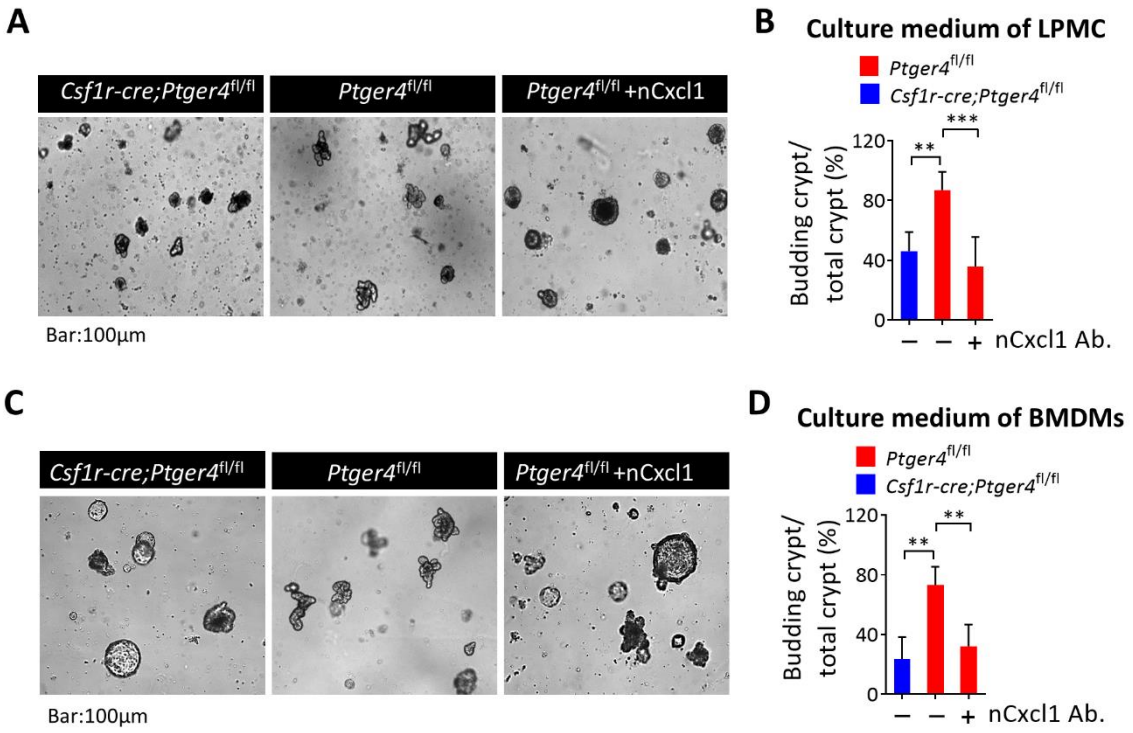

Figure 23. Cxcl1 production from EP4+ macrophages promote the intestinal epithelial regeneration

(A) The intestinal crypt organoids were cultured in differentiation medium containing the supernatant of LPMCs, which were isolated from colitis *Ptger4*$^{fl/fl}$ and *Csf1r-cre;Ptger4*$^{fl/fl}$ mouse. Cxcl1 neutralizing antibody (nCxcl1 Ab) were added to *Ptger4*$^{fl/fl}$ group. **(B)** Quantitative statistics of the number of budding crypts (D7) after incubation with supernatant of LPMCs (n=5-8. ***$P < 0.001$). **(C)** The intestinal crypt organoids were cultured in differentiation medium containing the cuture media of BMDMs, which were isolated from colitis *Ptger4*$^{fl/fl}$ and *Csf1r-cre;Ptger4*$^{fl/fl}$ mouse. Cxcl1 neutralizing antibody (nCxcl1 Ab) were added to *Ptger4*$^{fl/fl}$ group. **(D)** Quantitative statistics of the number of budding crypts (D7) after incubation with the cuture media of BMDMs (n=5-7. **$P < 0.01$).

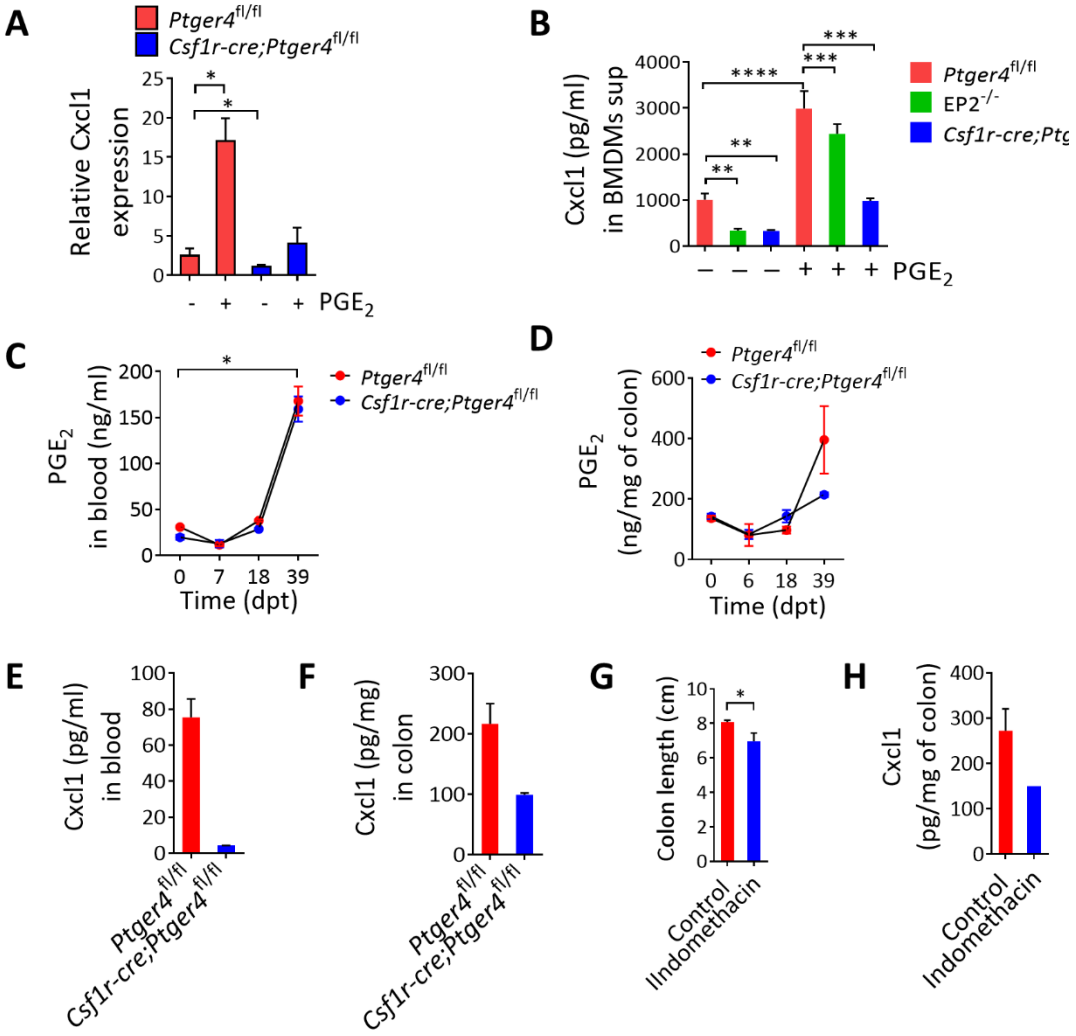

Figure 24. Increased Cxcl1 during the recovery phase is correlated with the increased PGE_2

(A) Gene transcripts of *Cxcl1* in BMDMs from *Ptger4*$^{fl/fl}$ and *Csf1r-cre;Ptger4*$^{fl/fl}$ mice determined using qPCR. BMDMs were treated with PGE_2 (10 μM) for 48 hours (n=5. **P* < 0.05). **(B)** Production of Cxcl1 levels in BMDMs of *Ptger4*$^{fl/fl}$, EP2$^{-/-}$ and *Csf1r-cre;Ptger4*$^{fl/fl}$ mice after 72 hours of PGE_2 treatment. (n=4. ***P* < 0.01, ****P* < 0.001, *****P* < 0.001). Production of PGE_2 levels was measured in sera **(C)** and colon lysate **(D)** of *Ptger4*$^{fl/fl}$ and *Csf1r-cre;Ptger4*$^{fl/fl}$ mice at indicated time points. Production of Cxcl1 levels in sera **(E)** and colon lysate **(F)** obtained from *Ptger4*$^{fl/fl}$ and *Csf1r-cre;Ptger4*$^{fl/fl}$

mice on day 35 as quantified by ELISA (n=3. *$P < 0.05$). **(G)** Colon length and **(H)** Cxcl1 levels in colon lysate and of day 21 DSS induced colitis mice received indomethacin in drinking water (n=3. *$P < 0.05$).

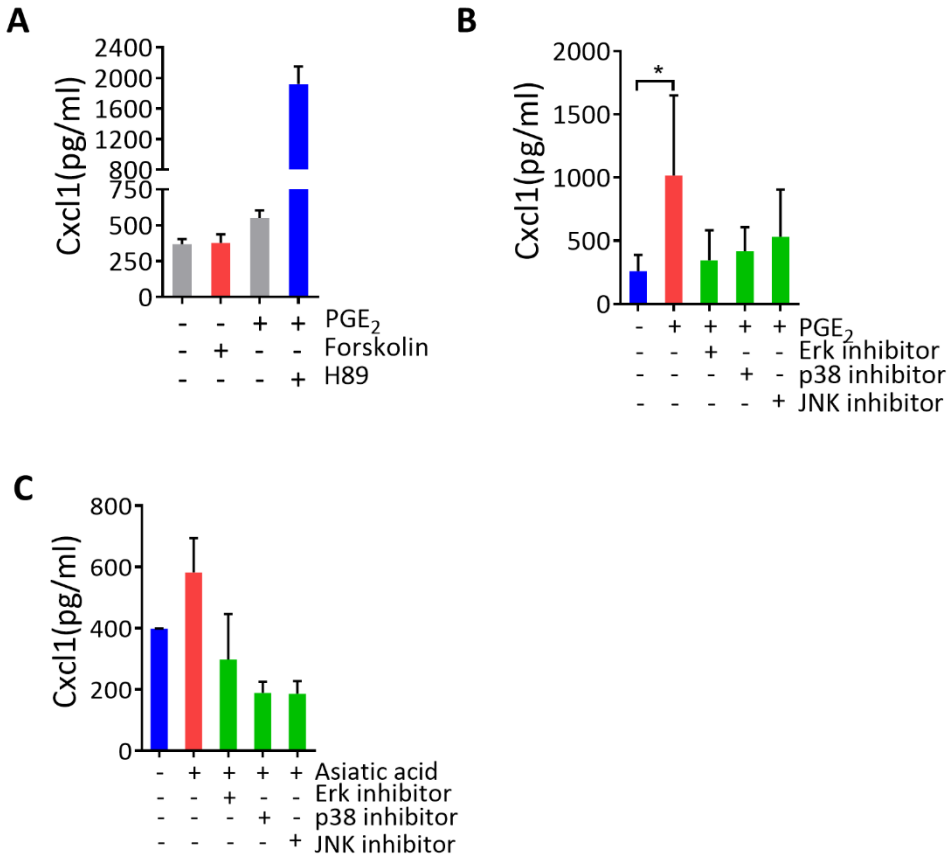

Figure 25. Cxcl1 is produced under the PGE_2/EP4/MAPKs axis in macrophages

Cxcl1 production by BMDMs determined by ELISA. (**A**) BMDMs were treated with 10 μM PGE_2 or 50 μM cAMP activator forskolin for 72 hours after pretreatment with 40 μM PKA inhibitor H-89. BMDMs were pretreated with 1 μM PD98059 (ERK inhibitor), 0.5 μM SB203580 (p38 inhibitor), or 0.5 μM SP600125 (JNK inhibitor) 1 hour before being treated with PGE_2 **(B)** or 20 μM Asiatic acid **(C)**.

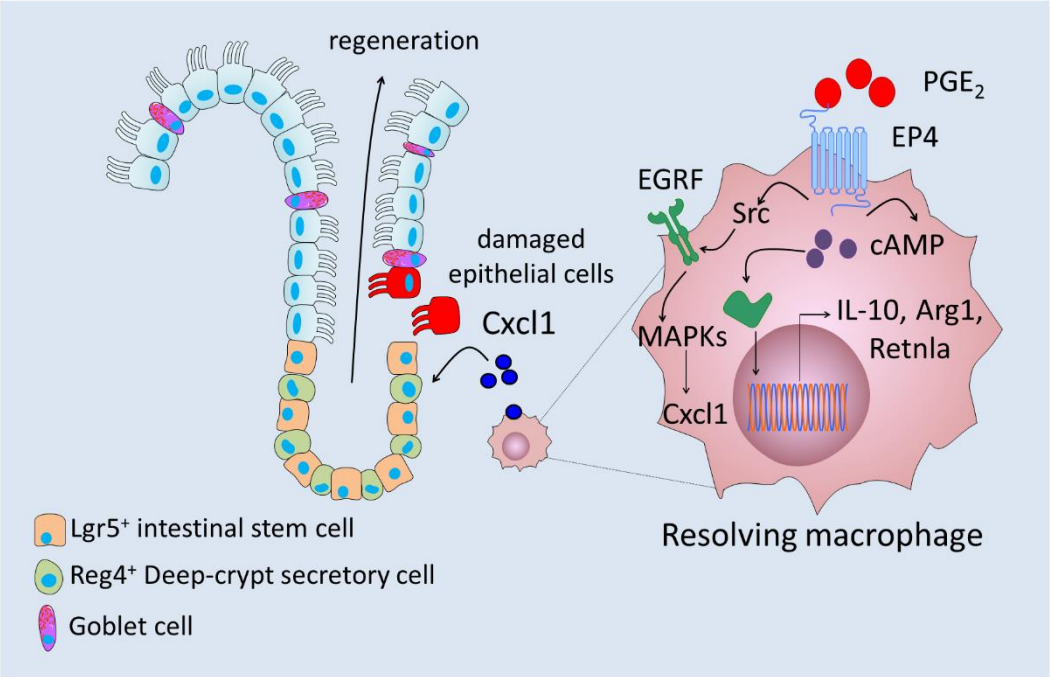

Figure 26. Schematic summary

PGE_2 potentiates anti-inflammatory phenotype of macrophage through EP4-cAMP-PKA cascade. macrophage EP4 signaling promotes the wound healing function of colonic macrophages by increasing IL-10, Arginase I and Retnla. Cxcl1 Production by macrophage EP4 dependent signaling promotes intestinal epithelial cell proliferation

DISCUSSION

In this study, I identified $EP4^+$ macrophages as the major inducer for the epithelial regeneration in a damaged intestine. EP4 expression of macrophages did not appear to be necessary for normal maintenance of crypts, because *Csf1r-cre;Ptger4*$^{fl/fl}$ colonic crypts had normal morphology. Nonetheless, my data indicated that EP4 expression of macrophages orchestrated the proliferation and survival of epithelial progenitors during resolving phase. Monocyte derived macrophages obtained wound healing phenotype in a EP4 dependent manner and was sufficient to promote expansion of crypt organoids, an effect mainly dependent on Cxcl1. PGE_2 was increased above the homeostatic level during the resolution phase of intestinal inflammation, contributing to the production of Cxcl1 from $EP4^+$ macrophages. Recent genome-wide association studies demonstrated a significant association of single-nucleotide polymorphisms within the proximity of the PTGER4 gene region, which regulate EP4 expression, with Crohn's disease (21). Apart from the previous studies demonstrating the pathogenesis of IBDs regarding PTGER4 SNPs, such as the EP4-mediated intestinal immune tolerance and maintaining mucosal integrity, my study presented here reveals an essential role of EP4 expressing macrophages on the mucosal wound healing, supporting a new idea on the treatment of such cases of IBDs (21, 22).

Many other studies indicate the formation, proper functioning, and survival of stem cells is strongly influenced by their local microenvironment (23, 24). In the intestine, several mesenchymal constituents form structural components of the intestinal stem cell niche (25). Subepithelial myofibroblasts migrate upward from the crypt base, placing them in strategic position to establish and maintain instructive communications with stem cells

and their descendants (26). A submucosal plexus of enteric neurons communicates with a subset of crypt epithelial progenitors in a growth factor-signaling pathway dependent manner(27). The microvasculature underlying the crypt base also effects stem cell survival. $CD34^+$ mesenchymal cells are a component of the intestinal stem cell niche after injury by producing Wnt2b, Grmlin1 and R-spondin1 (28). Activated macrophages also has been revealed as one of critical elements of the colonic epithelial stem cell niche necessary for regenerative responses to injury (29). Since this important study has been reported in 2005, several supporting mechanisms have been published so far. Wnt ligands are the most frequently mentioned effectors from macrophages, for example, macrophage derived extracellular vesicle-packaged Wnts rescue intestinal stem cells in radiation injury model (30). In addition, IL-4/STAT6-dependent Wnt productions from macrophages were critical in mucosal repair in 2,4,6-trinitrobenzene sulfonic acid (TNBS) induced colitis model (31). By contrast, I could not find significant difference of Wnt transcripts including Wnt2b, Wnt6, Wnt7b and Wnt10a between the intestinal *Ptger4*$^{fl/fl}$ macrophages and *Csf1r-cre;Ptger4*$^{fl/fl}$ macrophages from my RNA sequencing data (data not shown). Quiros *et al*. showed that macrophage derived IL-10 induced epithelial CREB activation and subsequence synthesis of the pro-repair WNT1-inducible signaling proteins 1 (WISP-1) followed by mucosal healing in punch biopsy model (32), however, IL-10 expression of macrophages was not significant different in WT and $EP4^{-/-}$ mice in this study. In addition, I could not observe a role of IL-4 in inducing $CD206^+$ macrophages in my colitis model, whereas Bosurgi *et al.* showed the increased CD206 expression by stimulation with concomitant IL-4 and apoptotic cells in DSS induced colitis model (33). One of the difference between these studies and my work is that I focused to investigate the phenotype of macrophages in the late recovery phase, whereas most of other studies performed their experiments at the inflammatory phase. None of other studies showed the

complete defect of wound healing in intestinal inflammation model distinct in contrast with my results, thus I am strongly convinced that PGE_2/EP4 axis in macrophages is a critical component of mucosal healing machinery.

PGE_2 is an eicosanoid that modulates diverse physiologic and pathologic functions. To avoid undesired effects associated with dysregulated inflammation, PGE_2 tissue concentrations are tightly regulated by expression of COX1 and COX2, mPGES1 biosynthetic enzymes, as well as degradative enzymes (15-PGDH). The COX1 and COX2 enzymes are responsible for the catabolism of arachidonic acid into PGH_2, the precursor of PGI_2, PGD_2, PGF2a, TxA_2 and PGE_2 (34). In a homeostatic state, intestine has the highest contents of PGE_2 among known other tissues such as lung, bone marrow and liver. COX2 and mPGES1 expressions mostly localize in the lamina propria, specifically abundant in monocyte/macrophages (35). During inflammation, contradicted data has been reported about the tissue level of PGE_2. Peng *et al.* showed that COX-1 and PGE_2 were significantly decreased in colon of UC patients and mice of DSS model (36), by contrast, Maseda *et al.* showed increased PGE_2 in colon from T-cell transfer mediated colitis model (35). Although with different model, Ho *et al.* also showed a surge of PGE_2 in damaged muscle tissue (8). In this study, I observed a slight decrease during inflammatory phase and a clearly increased PGE_2 both in colon and blood at the late resolving phase in my DSS-induced colitis model (Figure 25C-D). This means that a complete resolution to the homeostasis takes a time much more than I expected, and the reconstructed tissue components might increase PGE_2 production via high expressions of COXs and Ptges, further accelerating tissue regeneration.

The presence of $CD206^+$ regulatory macrophages were recently suggested as a prognostic factor in determining response rate to the anti-TNFα therapy in CD patients (37). Ipilimumab Fc portion mediated Fcγ receptor activation and the classical alternative activator IL-4 are known factors inducing $CD206^+$ macrophages (37), however, the reasons for how they are created in intestine is still not sufficiently understood. The strict correlation between EP4 and CD206 expression shown in this study thus identify a new mechanistic role of EP4 for inducing and maintaining $CD206^+$ macrophages which played a critical function in intestinal wound healing. EP4 expression on macrophages continued to increase during inflammation and peak at the resolution phase, rendering the full responsiveness to the increased PGE_2 which directly aided wound healing phenotype of macrophages via EP4 signaling pathway.

Several lines of evidence from clinical and animal model studies have shown that Cxcl1 plays a beneficial role by trafficking and activating neutrophils in response to infections (38-40). Cxcl1 produced by resident macrophages and/or epithelial cells rapidly travels to the bloodstream, where it orchestrates neutrophil trafficking from vasculature into the tissue (41, 42). Although Cxcl1 may be dangerous for treatment of colitis because of neutrophil trafficking, from my data that level of Cxcl1in colon or blood of *Csf1r-cre;Ptger4*$^{fl/fl}$ mice at 39 dpt was lower than that of naïve mice, I could predict that appropriate level of Cxcl1 needs to tissue regeneration during the resolution phase. Wang *et al.* identified mechanism that PGE_2 stimulates expression of the CXCL1 in colorectal cancer cells through activation of an the EGFR–MAPK cascade (43). I also observed similar mechanism that PGE_2/EP4/MAPK signaling axis involved in Cxcl1 production of macrophages. However, roles of Cxcl1 in the regulation of intestinal epithelial remains largely undefined. In this study, for the first time, I showed that Cxcl1

production from $EP4^+$ macrophages was necessary for the intestinal epithelial regeneration (Figure 24).

The treatment of EP4 agonist has shown to provide a beneficial effect in mice models of colitis (44) and in a Phase II trial with ulcerative colitis patients (45). Although the beneficial effects of EP4 agonists are likely mediated through multiple EP4-expressing cell types, my data suggests that EP4 expressing macrophages have a benefit on improved wound repair response of the intestinal epithelium. For future macrophage EP4 signaling-directed IBD therapeutics, one of the target drugs is MAPKs activator asiatic acid that result in increased Cxcl1 production of macrophages. It has been reported that asiatic acid ameliorated DSS-induced murine experimental colitis through inhibition of NLRP3 inflammasome activation (46). Targeted drug delivery to macrophages is therefore one of the remaining challenges to obtaining high drug efficacy without substantial adverse effects. For example, macrophage-targeting nanoparticles, such as mannosylated or folic acid conjugated liposomes, could be synthesized to deliver specific pathway inhibitors or agonists to promote differentiation of $CD206^+$ or folate receptor-positive (FR+) inflammatory myeloid cells into resolution macrophages in the colon (47).

In conclusion, the present study has revealed that the expression of EP4 on macrophages helps to maintain colonic epithelial barrier integrity, and recovers damaged mucosal by Cxcl1 up-regulation of PGE_2/EP4/MAPK signaling. These results suggest that EP4 signaling of macrophages has a favorable therapeutic effect on DSS-induced ulcerative colitis, supporting its future developments of clinical application in inflammatory bowel disease.

REFERENCES

1. Taniguchi K, Wu LW, Grivennikov SI, de Jong PR, Lian I, Yu FX, et al. A gp130-Src-YAP module links inflammation to epithelial regeneration. Nature. 2015;519(7541):57-62.
2. Neurath MF. New targets for mucosal healing and therapy in inflammatory bowel diseases. Mucosal Immunol. 2014;7(1):6-19.
3. Turner JR. Intestinal mucosal barrier function in health and disease. Nat Rev Immunol. 2009;9(11):799-809.
4. Leoni G, Neumann PA, Sumagin R, Denning TL, Nusrat A. Wound repair: role of immune-epithelial interactions. Mucosal Immunol. 2015;8(5):959-68.
5. Kaunitz JD, Akiba Y. Control of Intestinal Epithelial Proliferation and Differentiation: The Microbiome, Enteroendocrine L Cells, Telocytes, Enteric Nerves, and GLP, Too. Dig Dis Sci. 2019;64(10):2709-16.
6. Bonner GF, Fakhri A, Vennamaneni SR. A long-term cohort study of nonsteroidal anti-inflammatory drug use and disease activity in outpatients with inflammatory bowel disease. Inflamm Bowel Dis. 2004;10(6):751-7.
7. Basivireddy J, Vasudevan A, Jacob M, Balasubramanian KA. Indomethacin-induced mitochondrial dysfunction and oxidative stress in villus enterocytes. Biochem Pharmacol. 2002;64(2):339-49.
8. Ho ATV, Palla AR, Blake MR, Yucel ND, Wang YX, Magnusson KEG, et al. Prostaglandin E2 is essential for efficacious skeletal muscle stem-cell function, augmenting regeneration and strength. Proc Natl Acad Sci U S A. 2017;114(26):6675-84.
9. Miyoshi H, VanDussen KL, Malvin NP, Ryu SH, Wang Y, Sonnek NM, et al. Prostaglandin E2 promotes intestinal repair through an adaptive cellular response of the epithelium. EMBO J. 2017;36(1):5-24.
10. Zhang S, Liu Y, Zhang X, Zhu D, Qi X, Cao X, et al. Prostaglandin E2 hydrogel improves cutaneous wound healing via M2 macrophages polarization. Theranostics. 2018;8(19):5348-61.
11. Na YR, Jung D, Yoon BR, Lee WW, Seok SH. Endogenous prostaglandin E2 potentiates anti-inflammatory phenotype of macrophage through the CREB-C/EBP-beta cascade. Eur J Immunol. 2015;45(9):2661-71.
12. Kaneda MM, Messer KS, Ralainirina N, Li H, Leem CJ, Gorjestani S, et al. PI3Kgamma is a molecular switch that controls immune suppression. Nature. 2016;539(7629):437-42.
13. Barrett T, Wilhite SE, Ledoux P, Evangelista C, Kim IF, Tomashevsky M, et al. NCBI GEO: archive for functional genomics data sets--update. Nucleic Acids Res. 2013;41(Database issue):D991-5.
14. Chen S, Zhou Y, Chen Y, Gu J. fastp: an ultra-fast all-in-one FASTQ preprocessor. Bioinformatics. 2018;34(17):i884-i90.
15. Bray NL, Pimentel H, Melsted P, Pachter L. Near-optimal probabilistic RNA-seq

quantification. Nat Biotechnol. 2016;34(5):525-7.
16. Frankish A, Diekhans M, Ferreira AM, Johnson R, Jungreis I, Loveland J, et al. GENCODE reference annotation for the human and mouse genomes. Nucleic Acids Res. 2019;47(D1):D766-D73.
17. Bain CC, Scott CL, Uronen-Hansson H, Gudjonsson S, Jansson O, Grip O, et al. Resident and pro-inflammatory macrophages in the colon represent alternative context-dependent fates of the same Ly6Chi monocyte precursors. Mucosal Immunol. 2013;6(3):498-510.
18. Novak ML, Koh TJ. Macrophage phenotypes during tissue repair. J Leukoc Biol. 2013;93(6):875-81.
19. Krzyszczyk P, Schloss R, Palmer A, Berthiaume F. The Role of Macrophages in Acute and Chronic Wound Healing and Interventions to Promote Pro-wound Healing Phenotypes. Front Physiol. 2018;9:419.
20. Martinez FO, Gordon S, Locati M, Mantovani A. Transcriptional profiling of the human monocyte-to-macrophage differentiation and polarization: new molecules and patterns of gene expression. J Immunol. 2006;177(10):7303-11.
21. Prager M, Buttner J, Buning C. PTGER4 modulating variants in Crohn's disease. Int J Colorectal Dis. 2014;29(8):909-15.
22. Abreu MT. The genetics and pathogenesis of inflammatory bowel disease. Gastroenterol Hepatol (N Y). 2013;9(8):521-3.
23. Morrison SJ, Spradling AC. Stem cells and niches: mechanisms that promote stem cell maintenance throughout life. Cell. 2008;132(4):598-611.
24. Birbrair A. Stem Cell Microenvironments and Beyond. Adv Exp Med Biol. 2017;1041:1-3.
25. Santos AJM, Lo YH, Mah AT, Kuo CJ. The Intestinal Stem Cell Niche: Homeostasis and Adaptations. Trends Cell Biol. 2018;28(12):1062-78.
26. Pastula A, Marcinkiewicz J. Cellular Interactions in the Intestinal Stem Cell Niche. Arch Immunol Ther Exp (Warsz). 2019;67(1):19-26.
27. Walsh KT, Zemper AE. The Enteric Nervous System for Epithelial Researchers: Basic Anatomy, Techniques, and Interactions With the Epithelium. Cell Mol Gastroenterol Hepatol. 2019;8(3):369-78.
28. Stzepourginski I, Nigro G, Jacob JM, Dulauroy S, Sansonetti PJ, Eberl G, et al. CD34+ mesenchymal cells are a major component of the intestinal stem cells niche at homeostasis and after injury. Proc Natl Acad Sci U S A. 2017;114(4):E506-E13.
29. Pull SL, Doherty JM, Mills JC, Gordon JI, Stappenbeck TS. Activated macrophages are an adaptive element of the colonic epithelial progenitor niche necessary for regenerative responses to injury. Proc Natl Acad Sci U S A. 2005;102(1):99-104.
30. Saha S, Aranda E, Hayakawa Y, Bhanja P, Atay S, Brodin NP, et al. Macrophage-derived extracellular vesicle-packaged WNTs rescue intestinal stem cells and enhance survival after radiation injury. Nat Commun. 2016;7:13096.

31. Cosin-Roger J, Ortiz-Masia D, Calatayud S, Hernandez C, Esplugues JV, Barrachina MD. The activation of Wnt signaling by a STAT6-dependent macrophage phenotype promotes mucosal repair in murine IBD. Mucosal Immunol. 2016;9(4):986-98.
32. Quiros M, Nishio H, Neumann PA, Siuda D, Brazil JC, Azcutia V, et al. Macrophage-derived IL-10 mediates mucosal repair by epithelial WISP-1 signaling. J Clin Invest. 2017;127(9):3510-20.
33. Bosurgi L, Cao YG, Cabeza-Cabrerizo M, Tucci A, Hughes LD, Kong Y, et al. Macrophage function in tissue repair and remodeling requires IL-4 or IL-13 with apoptotic cells. Science. 2017;356(6342):1072-6.
34. Hanna VS, Hafez EAA. Synopsis of arachidonic acid metabolism: A review. J Adv Res. 2018;11:23-32.
35. Maseda D, Banerjee A, Johnson EM, Washington MK, Kim H, Lau KS, et al. mPGES-1-Mediated Production of PGE2 and EP4 Receptor Sensing Regulate T Cell Colonic Inflammation. Front Immunol. 2018;9:2954.
36. Peng X, Li J, Tan S, Xu M, Tao J, Jiang J, et al. COX-1/PGE2/EP4 alleviates mucosal injury by upregulating beta-arr1-mediated Akt signaling in colitis. Sci Rep. 2017;7(1):1055.
37. Koelink PJ, Bloemendaal FM, Li B, Westera L, Vogels EWM, van Roest M, et al. Anti-TNF therapy in IBD exerts its therapeutic effect through macrophage IL-10 signalling. Gut. 2019.
38. Strieter RM, Keane MP, Burdick MD, Sakkour A, Murray LA, Belperio JA. The role of CXCR2/CXCR2 ligands in acute lung injury. Curr Drug Targets Inflamm Allergy. 2005;4(3):299-303.
39. Balamayooran G, Batra S, Fessler MB, Happel KI, Jeyaseelan S. Mechanisms of neutrophil accumulation in the lungs against bacteria. Am J Respir Cell Mol Biol. 2010;43(1):5-16.
40. Bhatia M, Zemans RL, Jeyaseelan S. Role of chemokines in the pathogenesis of acute lung injury. Am J Respir Cell Mol Biol. 2012;46(5):566-72.
41. Ley K, Laudanna C, Cybulsky MI, Nourshargh S. Getting to the site of inflammation: the leukocyte adhesion cascade updated. Nat Rev Immunol. 2007;7(9):678-89.
42. Phillipson M, Heit B, Colarusso P, Liu L, Ballantyne CM, Kubes P. Intraluminal crawling of neutrophils to emigration sites: a molecularly distinct process from adhesion in the recruitment cascade. J Exp Med. 2006;203(12):2569-75.
43. Wang D, Wang H, Brown J, Daikoku T, Ning W, Shi Q, et al. CXCL1 induced by prostaglandin E2 promotes angiogenesis in colorectal cancer. J Exp Med. 2006;203(4):941-51.
44. Jiang GL, Nieves A, Im WB, Old DW, Dinh DT, Wheeler L. The prevention of colitis by E Prostanoid receptor 4 agonist through enhancement of epithelium survival and regeneration. J Pharmacol Exp Ther. 2007;320(1):22-8.
45. Nakase H, Fujiyama Y, Oshitani N, Oga T, Nonomura K, Matsuoka T, et al. Effect of EP4 agonist (ONO-4819CD) for patients with mild to moderate ulcerative colitis refractory to

5-aminosalicylates: a randomized phase II, placebo-controlled trial. Inflamm Bowel Dis. 2010;16(5):731-3.
46. Guo W, Liu W, Jin B, Geng J, Li J, Ding H, et al. Asiatic acid ameliorates dextran sulfate sodium-induced murine experimental colitis via suppressing mitochondria-mediated NLRP3 inflammasome activation. Int Immunopharmacol. 2015;24(2):232-8.
47. Na YR, Stakenborg M, Seok SH, Matteoli G. Macrophages in intestinal inflammation and resolution: a potential therapeutic target in IBD. Nat Rev Gastroenterol Hepatol. 2019;16(9):531-43.

국문 초록

장 조직이 손상되었을 때 장 상피세포 장벽의 회복은 장관내 미생물 균총을 격리하여 만성적인 염증이 일어나는 것을 막아준다. 따라서 장 조직의 재생이 제대로 일어나지 않으면 장관내 미생물에 대한 면역반응이 지속적으로 일어나 염증성 대장염을 야기하게 되며 질환으로부터의 완전한 회복을 위해서는 손상된 장 조직이 적절한 재생을 거쳐 해부학적 장벽을 형성해야 한다. 큰포식세포는 상처 치유의 기본적인 요소 중에 하나로 잘 알려져 있으나 장에 있는 큰포식세포의 조직 재생 능력에 기여하는 주요한 요소가 무엇인지에 대해서는 잘 알려져 있지 않다. 본 연구에서는 큰포식세포에서 지질매개인자인 PGE_2 의 수용체 중 하나인 EP4 수용체의 발현이 손상 받은 장 조직 재생에 핵심적으로 관여하는 것을 증명하였다. 먼저 큰포식세포 특이적으로 EP4 를 발현하지 않는 마우스 (Csf1r-Cre/Esr1EP4$^{fl/fl}$)를 제작하여 대장염을 일으킨 후 장염의 회복기에 여전히 짧은 장 길이 및 높은 질병 활성도 등을 확인하여 장염의 회복이 잘 일어나지 않음을 확인하였다. 또한 EP4 를 발현하는 큰포식세포는 CD206 를 높게 발현하고 있었으며 세포 내 cAMP 를 많이 발현하고 있었다. 이는 EP4 가 상처치유 큰포식세포 형성에 중요한 기능을 하고 있음을

암시하고 있다. 더 나아가 회복기 시기의 큰포식세포에 대한 대단위 유전체 분석을 통하여 EP4 신호전달 체계에 의한 큰포식세포의 조직재생능력 향상과 연관 있는 분자생물학적 기전을 확립하고자 하였다. 대단위 유전체 분석을 통하여 Cxcl1 의 발현이 Csflr−EP4$^{-/-}$ 마우스 유래 장 큰포식세포에서 크게 감소하는 것을 확인하였으며, Cxcl1 이 PGE_2/EP4/MAPK 신호전달 체계를 통해서 crypt 의 분열을 도와 장 상피세포 분열을 촉진시킬 수 있음을 확인하였다. 본 연구결과로 염증성 대장염 모델의 조직 수복 시기에 조직의 적절한 재생이 이루어지기 위하여 EP4 에 의한 큰포식세포의 PGE_2/EP4/MAPK 신호전달체계 활성이 필요함을 확인하고 장 손상에 대한 재생 유도 반응의 전체적인 세포간 네트워크에서 큰포식세포가 Cxcl1 생산을 통하여 관여하는 분자생물학적 기전을 새롭게 밝혔다.

주요어 : 염증성 대장염, E prostanoid receptor 4, 대식세포, 장 조직 재생, C−X−C motif chemokine 1.

학 번 : 2015−30542